# Global Journal of Structural Design and Construction

Jan – Apr 2025 Vol – 13 Issue – 1

ENRICHED PUBLICATIONS PVT. LTD
S-9, IInd FLOOR, MLU POCKET,
MANISH ABHINAV PLAZA-II, ABOVE FEDERAL BANK,
PLOT NO-5, SECTOR-5, DWARKA, NEW DELHI, INDIA-
110075,
PHONE: - + (91)-(11)-47026006

# Global Journal of Structural Design and Construction

## Aims and Scope

Global Journal of Structural Design and Construction is a peer reviewed journal published by Original Papers. It is one of the pioneering starts up journal in Civil and Structural engineering which receives high quality research works from researchers across the globe. The journal publishes original research and review papers falling within the broad field of Civil Engineering.

# Global Journal of Structural Design and Construction

# Global Journal of Structural Design and Construction

Jan -Apr 2025 Vol – 13 Issue - 1

# MAPPING SOIL ERSOION USING RUSLE, GIS AND REMOTE SENSING TECHNIQUES

**Nancy Yadav [1], Dr. K. K. Singh [2]**

[1]Student, [2](Professor,
National Institute of Technology Kurukshetra.

***Abstract***

*For the protection of the land from erosion, it is essential to measure and locate soil loss. Revised Universal Soil Loss Equation, RUSLE, can estimate soil erosion potential on cell-by-cell raster-based GIS data frame. For the present work, Hiran River at Patan, Madhya Pradesh was selected for estimation of soil loss. The study aimed for qualitative assessment of soil erosion prone areas by calculating soil loss using RUSLE. Models, like RUSLE, require less data making soil erosion estimation practicable within larger scales as monthly precipitation data; digital elevation model, soil map, land use and land cover types and slope length and steepness were used to determine the RUSLE values. One of the most important parameters of RUSLE is C factor that represents effects of vegetation and other land covers. Estimating C factor in this study involves the use of Normalized Difference Vegetation Index (NDVI), an indicator which shows vegetation cover, using the regression equation in Spatial Analyst tool of ArcGIS 10.1 software.The Quantitative assessment has effectively been accomplished by calculating rates of soil loss and developing soil loss severity maps of the study areas using soil loss equation model RUSLE. This study has demonstrated GIS as a valuable tool in determining soil erosion and assisting the estimation of soil loss.*

***Keywords** –NDVI, RUSLE, Raster, GIS.*

## Introduction

Since the last centuries, soil erosion accelerated by human activities has become a serious environmental problem causing diverse environmental impacts by negatively affecting agricultural productivity, water supply and reservoir storage capacity. The risk of soil loss varies according to the configuration of the watershed, soil characteristics, climatic conditions and land use and management practices. Estimation of soil loss is usually difficult due to the complex intermesh of many factors, such as climate, soil, topography, land cover, and human interruptions. The models developed for estimating soil erosion can provide a better perceptive of natural phenomena such as transport and deposition of sediments. The Soil erosion models are widely used to estimate the erosion rates and makes use of mathematical expressions to symbolize the relationships between the factors and different processes of the environment. Several models have been proposed to describe and predict soil loss by water and sediment yield and considerably vary in their objectives, time and spatial scales. These models can be grouped into empirical models and physical process based models. Some of the physical based and empirical models include AGNPS, ANSWERS, WEPP and the Universal Soil Loss Equation (USLE), Modified Universal Soil Loss Equation (MUSLE), Revised Universal Soil Loss Equation (RUSLE) respectively.

In order to estimate the soil erosion, RUSLE has been applied to this case study. The use of Remote Sensing (RS) and GIS provide spatial input data, while RUSLE can be used to estimate the soil loss from the watershed. RUSLE, were selected to quantify the soil erosion rates because (1) data requirements are not too complex or unobtainable, (2) the models show compatibility with Geographical Information System(GIS), and (3) they are easy to understand and implement from a functional frame of reference.

One of the major deficiencies in the application of erosion models is the low availability of input data for the models. The traditional methods proved to be too costly and time consuming for generating this input data for the models. Extracting the spatial information on input parameters has become more easy and profitable with the help of remote sensing technology. However, the powerful spatial processing capabilities of Geographic Information System (GIS) and its compatibility with remote sensing data have made the soil erosion modelling advents more absolute and robust. The combined use of remote sensing and GIS could help to assess soil loss at various scales and identify areas that are at potential risk of soil erosion from the watershed. Thus, the integrated use of GIS and RUSLE has been proved to be an effective approach for estimating the significance and spatial distribution of erosion. The objectives of this study includes quantifying the soil loss, specifying main factors affecting the development of erosion and generating soil erosion maps for the study area.

## II. Study Area

The river "Hiran" is one of the north flowing tributary of Narmada. River Narmada is an important river as it happens to be the most sacred of the five holy rivers of India and is also referred to as the lifeline of Madhya Pradesh. Hiran River rises in the Bhanrer range in the Jabalpur district of Madhya Pradesh near the Kundam village at an elevation of 600 m. The source of **Hiran River** is the **Hiran Kund** in Kundam. Hiran flows generally in a south-westerly direction for a total length of 188 km to join the Narmada. Hiran being the biggest right bank tributary of the Narmada drains a total area of about 4648.85 sq.km.

For the present study the drainage area called as "Hiran" basin is selected on the River Narmada. The catchment is spread over Patan, a town in Jabalpur district in Madhya Pradesh. Spatial extent of Hiran basin is between 79°17'57.56"N to 80°9'0.60"N Latitudes and 23°7'10.65"E to 23°46'15.19"E Longitudes. The location map of the study area is shown in Fig.1.

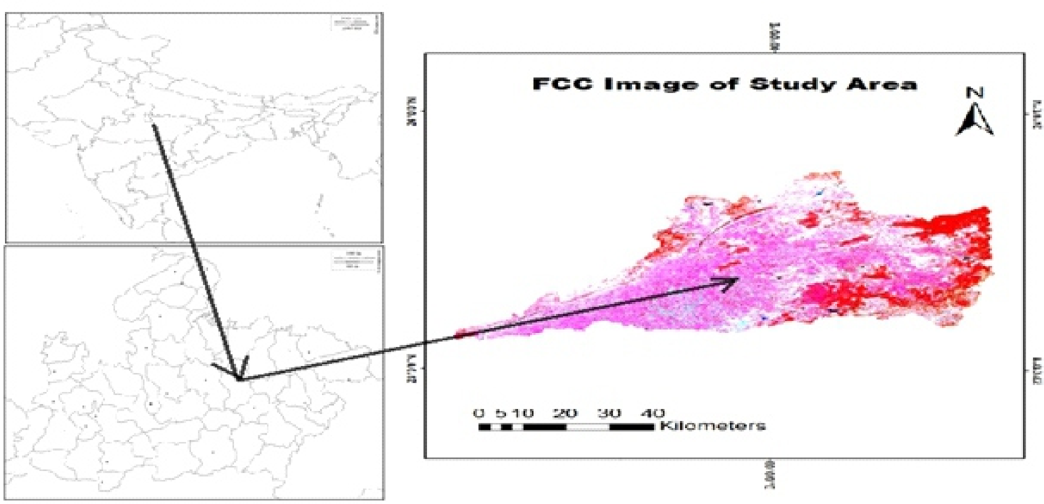


**Figure 1** Location map and FCC Image of the study Area

## III. Materials and Methods

The RUSLE equation is a Multiplication of five factors controlling the rill and inter-rill erosion (Renard et al., 1997) and expressed as:

$$A = R*K*LS*C*P \ldots\ldots\ldots. (1)$$

Where,

A is the mean annual soil loss expressed in ton\ha*yr.

R is rainfall and runoff erosivity index (in MJ* mm\ha*yr.)

K is soil erodibility factor (in ton*ha*h/ha*MJ*mm)

LS is slope Steepness and slope Length factor (dimensionless)

C is the cover factor (dimensionless)

P is the conservation practice factor (dimensionless).

For the estimation of soil erosion in this study, the rainfall data of 5 years were procured from the Collectrate Office, Municipal Department, Jabalpur from which the rainfall runoff erosivity factor (R-factor) was estimated. The soil map of the study area was procured and extracted from the World Soil Map. The soil erodibility factor (K-factor) map was then digitised and prepared in ArcGIS using the soil map extracted and the values of K-factor were assigned to the different soil types in the region. The Aster DEM with 90m spatial resolution was used to prepare the slope map and the flow accumulation map of the study area. The errors in the Aster DEM were rectified using the fill tool and the corrected DEM was utilized to derive the flow direction to prepare the flow accumulation map. These slope and flow accumulation maps were then used for preparing the LS factor map using raster calculator in ArcGIS. The C-factor map was prepared using NDVI Maps of 5 (2008-12) years. The land use landcover (LU/LC) map was procured from the Landsat LULC Map which provided accurate mapping of different LU/LC categories due to its high spatial resolution. The LU/LC map was used for preparing the conservation practice factor (P-factor) map and the values of P-factor were assigned to the different features based on the soil conservation practices taken up in the study area.

All the five parameter maps (having the same coordinate system) were converted to grid with 90m x 90m cell size (so as to maintain uniform cell size at par with spatial resolution of Aster DEM). The layers were then overlaid and multiplied pixel by pixel, using Equation 1, to estimate the soil erosion. Raster Calculator was used to build the expression: R * [K] * [C] * [P] * [LS] which, when applied to all cells in a raster scale, gives a map of average annual soil erosion.

## III. Results and Discussion

The soil erosion was calculated by overlaying the input parameters (R, K, LS, C, and P) by using RUSLE model with the help of GIS.

***A. R-Factor (Rainfall Runoff Erosivity Factor)***

The R factor i.e. erosivity index, the active force of the rain which cause detachment and transport of soil particles. For Indian conditions a linear relationship was developed by Ram Babu et al (2004) between average annual and seasonal (June-September) rainfall and Rainfall Erosivity factor (R). Derived relationships were as follows:

Annual relationship

Ra = 81.5 + 0.380 Pa.......(2)

Seasonal relationship

Rs = 71.9 + 0.361 Ps........(3)

Where,

$R_a/R_s$ = average annual/seasonal erosion index,

Pa = average annual rainfall (mm) and

Ps = average seasonal rainfall (mm).

For the present study eq. (2) is used to compute annual values of R-factor of the study area. Annual values of erosive factors from year 2008 to year 2013 for both monsoon and non-monsoon months are calculated using the equation 2. The rainfall data in basin is available at five different locations and are distributed so that the spatial variability of factor-R within the catchment is considered. The computed values of R-factor are presented in Table 5.1.

**Table 1** Rainfall Erosivity (R) Factors of Basin for different years

| S.no. | Year | Rainfall Erosivity |
|---|---|---|
| 1 | 2008 | 613.118 |
| 2 | 2009 | 610.975 |
| 3 | 2010 | 675.157 |
| 4 | 2011 | 752.841 |
| 5 | 2012 | 625.373 |
| 6 | 2013 | 904.635 |

***B. K-Factor (Soil Erodibility Factor)***

This factor computes the cohesive character of a soil type and its resistance to dislocate and transport due to raindrop impact and overland flow shear forces. The K-factor is determined for a particular soil type and reflects the physical and chemical properties of the soil, contributing to its erodibility potential. Thus, the area under study has 2 types of soil viz., loamy and clay. To estimate the K factor values, five characteristics of the soil - the relative percent of silt, sand, clay, percent organic matter, soil structure and soil permeability are required. K is assumed to be constant in RUSLE. For the present study, K-factor values are added in the attribute table of digitized soil map and finally K-map generated in ArcGIS using this attribute information. The values of K factor ranges from 0.0713351 to 0.0174614 and the map is shown in Fig.2.The K factor values do not present a very high variability; this may be due to the homogeneity of soil types and characteristics in the study area.

### *C. LS Factor (Slope Length Factor)*

The topographic factor is a very important parameter in soil erosion, since the gravity force is playing an important role in surface runoff. Thus, the*LS* factor for RUSLE is computed using the raster calculator in Arc Map to build an expression for estimating *slope length factor*, based on flow accumulation and slope steepness which is also used in this study. With the incorporation of Digital Elevation Models (DEM) into GIS, the slope gradient (*S*) and slope length (*L*) may be determined accurately and in RUSLE both the factors *L* and *S* are combined to give the topographic factor *LS*. Fig.3 showing the LS factor Map of the study area.

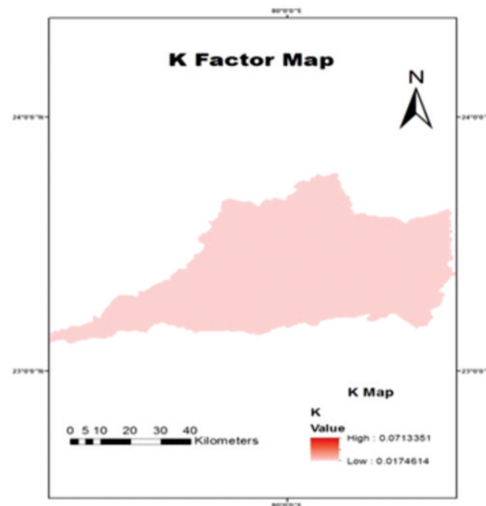


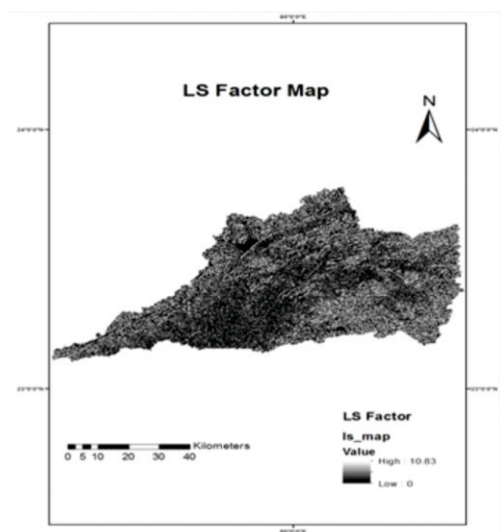


**Figure 2**K Factor Map of the Study Area**Figure 3**LS Factor Map of the Study Area

### *D. C- Factor (Land Cover and Management Factor)*

The land cover and management factor represent the effects of vegetation, soil erosion control practices and management and its value of which ranges from 0 in water bodies to slightly greater than 1 in barren lands. This factor is defined as the ratio ofsoil loss from cropped land under specific conditions to the correspondingloss from clean-tilled fallow land (Wischmeier and Smith, 1978).The Normalized Difference Vegetation Index (NDVI), an indicator of the vegetation vigor and health is used to generate the C-factor value for the study area. The NDVI maps can be analysed to formulate the linear equation between NDVI and RUSLE C-factor. The NDVIvalues less than zero (0) indicate the water and ice, so the negative values should not be considered in preparing the C factor equation. With these boundary conditions, the regression equation for C factor can be developed.

$$C_i = 0 \text{ If } NDVI < 0$$

$$C_i = -\left(\frac{1}{NDVI_{max}}\right)(NDVI_i) + 1 \text{ If } 0 < NDVI$$

These NDVI maps are used in determining the C factor maps according to the given conditions for year 2008 to 2013.

### *E. P-Factor (Erosion ControlPractice Factor)*

P is the factor that reflects the impact of support practices and considers any practice applied by humans to reduce erosion and the average annual erosion rate. P factor map was prepared from Land use/landcover map and is used for understanding the conservation practices in the study area.The P-factor value and the spatial distribution of P – factor is shown in Table 3 and Fig. 5.

**Table 2**Erosion Control Practice Factor

| S. No. | Class name | Conservation practice (P) |
|---|---|---|
| 1 | Water | 0 |
| 2 | Woodland | 0.8 |
| 3 | Wooded grassland | 0.8 |
| 4 | Closed grassland | 1 |
| 5 | Open grassland | 1 |
| 6 | Grassland | 0.7 |
| 7 | Cropland | 0.35 |
| 8 | Bare ground | 1 |

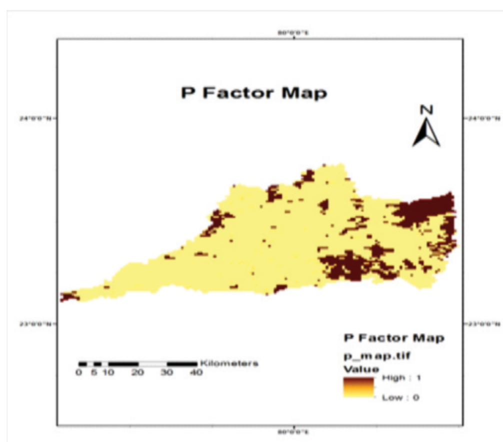


**Figure 4** Conservation Practice Factor Map of the study area

*Preparation of Erosion Map*

After assigning values to all the RUSLE parameters, R, K, LS, C, P, the respective maps were converted from vector to raster format keeping the cell size and projection uniform. These factor maps were then overlaid in raster calculator using the RUSLE Equation 1 and are shown below in fig.

**Table 3** Comparison of Observed and computed sediment loss for the Hiran River

| Year | Observed Mean Soil loss(tons/ha/yr) | Computed Mean Soil loss(tons/ha/yr) | Percent deviation |
|---|---|---|---|
| 2008 | 2.547 | 2.8057 | 10.15 |
| 2009 | 2.67 | 2.1863 | 18.3 |
| 2010 | 2.352 | 2.7210 | 15.69 |
| 2011 | 2.527 | 3.2536 | 10.20 |
| 2012 | 2.4202 | 2.7907 | 15.30 |

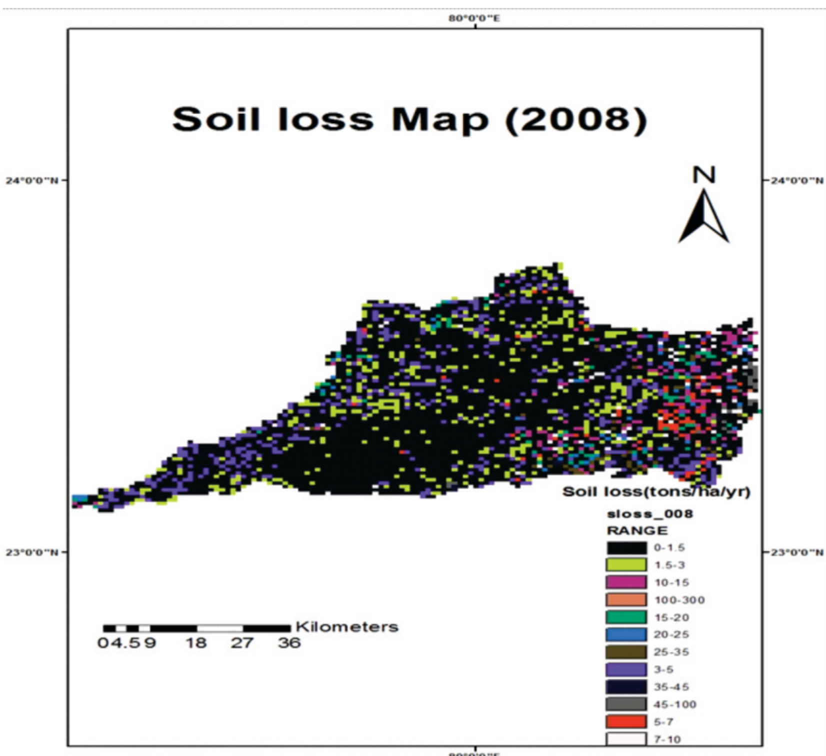


**Figure 5** Soil loss Map for 2008

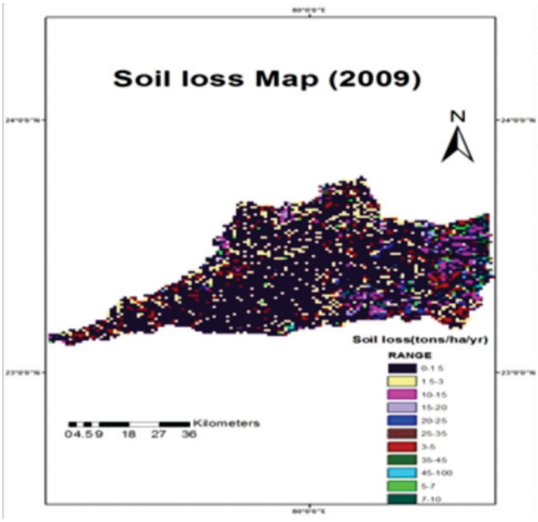


Fig 6. Soil loss Map for 2009

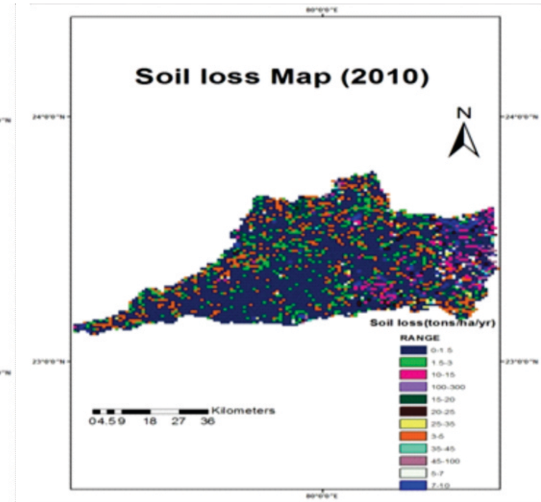


Fig 7. Soil loss Map for 2010

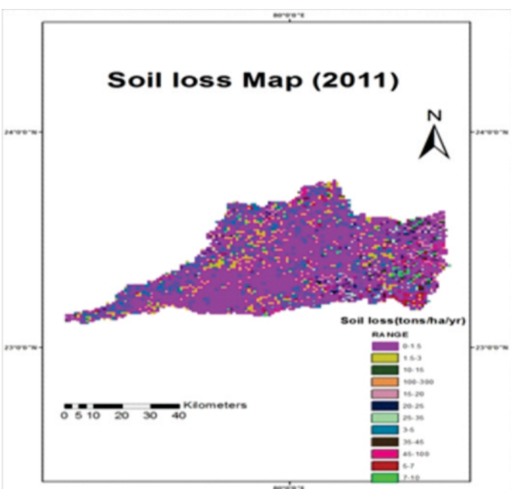


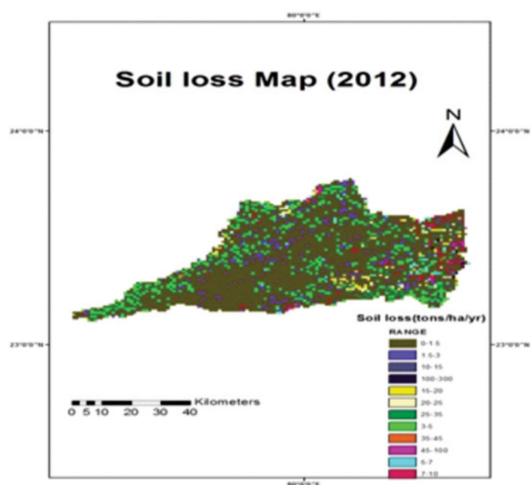


**Fig 8** Soil loss Map for 2011**Fig 9**Soil loss Map for 2011

**Conclusions**

In the present study, the RUSLE model adopted for estimating the annual average soil loss in the Hiran river watershed provided satisfactory results, and it can be effectively used for estimating soil erosion in similar other micro watersheds. The average annual soil loss in the Hiran river watershed using the RUSLE method was found to be 2.8057, 2.1863, 2.7210, 3.2536, 2.7907 tons ha-1 yr-1 for 2008-2012 respectively.

The use of GIS, and remote sensing data enabled the accurate determination of the spatial distribution of the RUSLE parameters. The creation of database through conventional methods is time consuming, and costly. Thus, remote sensing and GIS can play significant role in generation of input parameters for inaccessible areas of the watershed where ground based observations are difficult for the soil erosion modelling.

## References


[1] Rabia, A.H.(2012). *Mapping Soil Erosion Risk Using Rusle, Gis and Remote Sensing Techniques*. The 4th International Congress of ECSSS, EUROSOIL, Bari, Italy.

[2] Adediji, A.,Tukur,A.M., and Adepoju, K.A. (2010). *Assessment of Revised Universal Soil Loss Equation (RUSLE) in Katsina Area, Katsina State of Nigeria using Remote Sensing (RS) and Geographic Information System (GIS).* Iranica Journal of Energy & Environment 1 (3): 255-264.

[3] Alejandra, M. *Soil Erosion Calculation using Remote Sensing and GIS in Río Grande de Arecibo Watershed, Puerto Rico.*

[4] Alejandro, M. (2007). *Estimation of vegetation parameter for modelling soil erosion using linear Spectral Mixture Analysis of Landsat ETM data.* ISPRS Journal of Photogrammetry & Remote Sensing 62, 309–324.

[5] Tirkey, A.S., Pandey, A.C., andNathawat, M.S. (2013). *Use of Satellite Data, GIS and RUSLE for Estimation of Average Annual Soil Loss in Daltonganj Watershed of Jharkhand (India).* Journal of Remote Sensing Technology, Vol. 1 Iss. 1, PP. 20-30.

[6] Elangovan, A.B., and Seetharaman, R. (2011). *Estimating Rainfall Erosivity of the Revised Universal Soil Loss Equation from daily rainfall depth in Krishanagiri Watershed region of Tamil Nadu, India*. 2011 International Conference on Environmental and Computer Science IPCBEE vol.19.

[7] Pandey, A., Chowdary, V. M., andMal, B. C. (2007). *Identification of critical erosion prone areas in the small agricultural watershed using*

*USLE, GIS and remote sensing*",Water Resour Manage 21:729–746.

[8] Fernandez,C., Wu, J.Q., McCool, D.K. and Stockle,C.O. (2003). *Estimating water erosion and sediment yield with GIs, RUSLE, and SEDD. Journal of Soil and Water Conservation*58(3):128-136.

[9] Cohen, M.J., Shepherd, K.D., and Walsh, M.G.(2004). *Empirical Reformulation of the Universal Soil Loss Equation for Erosion Risk Assessment in a Tropical Watershed*. Geoderma124:235-252.

[10] Ouyang, D., and Bartholic,J.*Predicting Sediment Delivery Ratio inSaginaw Bay Watershed.* Institute of Water Research, Michigan State University, East Lansing, MI.

[11] Jaramillo, F. (2007) *Estimating and modelling soil loss and sediment yield in the Maracas-St. Joseph River Catchment with empirical models (RUSLE and MUSLE) and a physically based model (Erosion 3D)*. Civil and Environmental Engineering Department McGill University, Montreal.

[12] Sharma, G., and Goyal, R. (2013). Qualitative and Quantitative Soil Erosion Mapping of Micro-watersheds of Bisalpur Reservoir using Remote sensing and GIS. UIM-2013, NRSC ISRO.

[13] Foster, G.R.,Weesies, G.A.,McCool, D.K.,Yoder,D.C., andRenard, K.G.,(1999). *Revised Universal Soil Loss Equation USER'S MANUAL.*

[14] Naqvi, H.R., Devi, L.M., and Siddiqui, M. A.(2012).*Soil Loss Prediction and Prioritization Based on Revised Universal Soil Loss Estimation (RUSLE) Model Using Geospatial Technique*. International Journal of Environmental Protection, Vol. 2 No. 3, PP. 39-43.

[15] Ahmad, I., and Verma,M. K.(2008). *Application of USLE model and GIS in estimation of soil erosion for Tandula Reservoir*. International Journal of Emerging Technology and Advanced Engineering Volume 3, Issue 4.

[16] Blaszczynski, J. (2003). *Estimating Watershed Runoff and Sediment Yield Using a GIS Interface to Curve Number and MUSLE Models.* National Science and

Technology Center, Resource notes 66.

[17] Jayarathne, K.D.B.L.,Dayawansa, N.D.K., and De Silva,R. P.(2010). *GIS Based Analysis of Biophysical and Socio - Economic Factors for Land Degradation in Kandaketiya DS Division*. Tropical Agricultural Research Vol. 21(4): 361 – 367.

[18] Renard, K.G., Foster, G.R., Weesies, G.A. and Porter, J.P. (1991). *Revised universal soil loss equation*. Journal of Soil and Water Conservation, Volume 46. Number 1.

[19] Jain, M.K., and Kothyari, U.C.(2009) *Estimation of soil erosion and sediment yield using GIS*. Hydrological Sciences Journal, 45:5, 771-786.

[20] Rinos, M. H. M., Aggarwal,S. P. and De Silva, R.P.(2014) *Application of Remote Sensing and GIS on soil erosion assessment at Bata River Basin, India*.

[21] Alkharabsheha, M.M., Alexandridisa, T.K.,Bilasb, G., Misopolinosb, N., andSilleosa, N. (2013) *Impact of land cover change on soil erosion hazard in northern Jordan using remotesensing and GIS*. Procedia Environmental Sciences 19. 912 – 921.

[22] Kinnell, P.I.A. (2010) *Event soil loss, runoff and the Universal Soil Loss Equation family of models: A review*. Journal of Hydrology 385, 384–397.

[23] Dabral P. P., Baithuri,N., and Pandey, A. (2008)*Soil Erosion Assessment ina Hilly Catchment of North Eastern India Using USLE, GIS and Remote Sensing*. Water Resource Manage 22:1783–1798.

[24] Singh, R., and Phadke, V.S. (2006) *Assessing soil loss by water erosion in Jamni river basin, Bundelkhand region, India, adopting USLE using GIS*. Current Science, Vol. 90, No.10.

[25] Efe, R., Ekinci, D., and Curebal, I.*Erosion Analysis of Fındıklı Creek catchment(Northwest of Turkey) using GIS based on RUSLE (3D) Method*. Fresenius Environmental Bulletin, 17(2), 576-586.

[26] Parveen, R., and Kumar, U. (2012). *Integrated Approach of Universal Soil LossEquation (USLE) and Geographical Information System (GIS) for Soil

*Loss Risk Assessmentin Upper South Koel Basin, Jharkhand* Journal of Geographic Information System, 4, 588-596.

[27] Arekhi, S., Shabani, A., and Rostamizad, G. (2011). *Application of the modified universal soil loss equation (MUSLE) in prediction of sediment yield (Case study:Kengir Watershed, Iran*). Saudi Society for Geosciences 2010.

[28] SADEGHI, S. H. R.,and MIZUYAMA, T. (2010). *Applicability of the Modified UniversalSoil Loss Equation for prediction of sediment yield in Khanmirza watershed, Iran* Hydrological Sciences Journal 52(5).

[29] Sharma,S.K., Gajbhiye, S., Nema,R.K., and Tignath,S. (2014). *Assessing Vulnerability toSoil Erosion of a Watershed of Tons River Basin in Madhya Pradesh using Remote Sensingand GIS* International Journal of Environmental Research and Development.ISSN 2249-3131 Volume 4, Number 2, pp. 153-164.

[30] Biswas, S. (2012)*Estimation of Soil Erosion using Remote Sensing and GIS and Prioritization of Catchments* International Journal of Emerging Technology and Advanced Engineering, Volume 2, Issue 7.

[31] Kumar, S., and Kushwaha, S.P.S. Modelling *soil erosion risk based on RUSLE-3D using GIS in a Shivalik sub-watershed.* J. Earth Syst. Sci. 122, No. 2, pp. 389–398.

[32] Prasannakumar, V., Vijith, H., Abinod, S., and Geetha, N. (2012) *Estimation of soil erosionrisk within a small mountainous sub-watershed in Kerala, India, using Revised UniversalSoil Loss Equation (RUSLE) and geo-information technology* Geoscience Frontiers3(2) (2012) 209-215.

# SWAT MODEL ASSESSMENT OF HYDROLOGICAL IMPACTS OF HRU-SCALE INVASION BY *PARTHENIUM HYSTEROPHORUS* WEED

**Soham Adla** [1], **Shivam Tripathi** [2]

[1,2]Department of Civil Engineering,
Indian Institute of Technology Kanpur.

***Abstract***

*Parthenium hysterophorus is a notorious invasive alien species with an increasing presence in India attributed to its high growth rate due to its ability to compete against many native species and adaptability to varied environmental conditions. Despite extensive studies on its impacts on human health, livestock, agricultural productivity, and infestation mitigation techniques, there have been few studies highlighting its hydrological impact on components of the water balance at any scale. This study used the physically based SWAT (Soil and Water Assessment Tool) model to simulate Parthenium invasions at the scale of a hydrologic response unit (HRU) – the smallest user defined homogenous unit of computation within the SWAT model. The primarily agricultural basin of the Punpun river in Bihar was chosen as the study area, fallow land and kharif crop HRUs were infested with Parthenium, and results were analysed across soil type and slope classes. SWAT modeled higher (but statistically insignificant) levels of ET losses for Parthenium compared to both the native LUs, subject to soil moisture availability which was a limiting factor for ET during the dry season. Average monthly soil moisture levels were correspondingly and consistently slightly lower for Parthenium contradicting heuristic experience of local water managers. The study highlights the need for localized measurement of crop parameters to resolve such contradictions.*

**Keywords:** *Parthenium Hysterophorus; SWAT; HRU; water balance; invasive alien species*

## Introduction

*Parthenium Hysterophorus* is an invasive alien plant species in India. It has invaded about 2 million hectares of agricultural land, mainly in Punjab, Haryana and Uttar Pradesh (Dwivedi et al. 2009) because of its high germination capacity, ability to withstand and grow in diverse climatic and soil conditions, and allelopathic ability to restrict the growth of native plant species. Its spread may result in impacts on human health on exposure (Patel 2011), decrease in crop productivity and harmful impacts on livestock and biodiversity (Kumari 2014).

### *1.1 Motivation*

The increasing spread of*Parthenium Hysterophorus* weed in the fertile crop-producing plains of North India, particularly in the Ganga basin, is critical not only from the perspective of its impacts on human and animal health and inhibitory effects on crop productivity, but also in terms of potentially significant impacts on the water resources of the infested catchment, by influencing the water balance components.

A study by Adla and Tripathi (2014) used the Soil and Water Assessment Tool (SWAT) model (Arnold et al. 1998) to investigate the basin scale hydrological effects of an invasion by *Parthenium Hysterophorus*. The land use of the primarily agricultural Punpun river basin (Bihar) was modified under the framework of spatially random scenarios of incremental *Parthenium* cover, representative of increasing extents of a hypothetical invasion. Results indicated that the while the presence of *Parthenium* did not alter the annual water balance significantly, an increasing land cover reduced evapotranspiration (ET) losses which subsequently led to higher soil moisture buildup before the onset of the monsoon. The study, however, had a few limitations.

The plant parameters of*Parthenium* used in the SWAT model were derived from a combination of existing literature (Pandey et. al 2003) and *in-situ* measurements which implied that the parameter estimates were not internally consistent, and did not follow the standards for SWAT model plant parameter estimation. It was assumed that the *kharif* crop was rain-fed, and hence irrigation inputs were excluded from the model setup. On request, the USDA-ARS (US Department of Agriculture – Agricultural Research Service) has developed an official set of *Parthenium* plant parameters now included within the SWAT model by default. In this study, irrigation has been incorporated realistically as a management practice during the *kharif* cropping season. However, the major conceptual limitation of the previous study was that a model had been constructed to simulate a river basin scale invasion by *Parthenium*. Since regular agricultural management practices by farmers (applying weedicides, manual uprooting etc.) preclude any fully basin scale invasions of agricultural land by most invasive species, the study of Adla and Tripathi (2014) was not representative of actual conditions on the ground, but served to provide an overall perspective of the hydrological impacts of such an extensive land use change at the intra-annual time scale. Also, such an approach implied challenges in isolating the particular processes through which this land use change may have causally impacted water balance variables. The framework of the land use change deployed in the present study can potentially circumvent this limitation and isolate the drivers of changes in the water balance, by simulating *Parthenium* invasions at the scale of a hydrologic response unit (HRU) – the smallest user defined homogenous unit of computation within the SWAT model. As invasion at the scale of HRU is representative of the scale of an actual invasion, the use of the LU-split option in SWAT can establish a common ground for comparing the native and invaded land covers and their hydrological effects.

### *1.2 Objectives*

The objective of the study was to simulate invasions by *Parthenium Hysterophorus* at management-appropriate scales of HRUs, the basic computational units in the SWAT model. Each HRU had a unique combination of native land cover, soil type and slope category. A subsequent partial invasion of each such HRU would then help to detect the marginal effect of a *Parthenium* invasion. The study aimed at fulfilling the following objectives:

1. To construct a representative hydrological model of the Punpun river basin by using the SWAT model.
2. To simulate invasions by *Parthenium Hysterophorus* at the HRU-scale
3. To quantify and explain the impacts of invasion by *Parthenium Hysterophorus* on the water balance components at annual and intra-annual levels.

## 2. Materials and Methods

### 2.1 *The SWAT Model*

The Soil and Water Assessment Tool (SWAT) Model (Arnold et al. 1998) is a semi-distributed river basin model which simulates water, sediment, nutrient and point-source pollution yields at a daily time step (Gassman et al. 2007). It was developed through by USDA to assist water resource managers in assessing impacts of land-use management on water and diffuse pollution for large ungauged catchments with different soil types, land uses and management practices (Arnold and Fohrer 2005).

The SWAT model framework divides the catchment into multiple sub-basins, each of which is further subdivided into hydrologic response units (HRUs). An HRU is the smallest unit of computation in the SWAT model. It does not have any spatial reference (the sub-basin is the smallest unit with spatial meaning) and has a unique combination of land use, soil and slope class characteristics, which can be modified by user inputs. The SWAT model computes the daily water balance for each HRU in the model according to Equation 1:

$$\Delta\,(\text{Storage}) = \Delta(\text{SHow})\,n + \Delta\,(\text{Sh.Aq}) + \Delta\,(\text{Dp.Aq}) + \Delta\,(\text{Surf\_daylog}) + \Delta\,(\text{Lat\_daylog})$$

where *Storage* is the sum of all storage terms, *Snow* is the amount of water stored as snow, *SW* is the amount of water stored in the soil profile on a given day, *Sh.Aq* is the depth of water in the soil aquifer, *Dp.Aq* is the depth of water in the deep aquifer, *Surf_daylag* is the amount of surface runoff lagged over a day, *Lat_daylag* is the amount of lagged lateral flow, and Δ represents the change in each of the terms over a daily time step. The water losses are computed according to Equation 2:

$$\text{Waterloss} = \text{Pcp}_{day} + \text{Irr}_{day} - \text{Surf}_{day} - \text{Lat}_{day} - \text{ET}_{day} - \text{GWQ}_{day} - \text{Rvap}_{day} -$$

$Rchrg_{day}$ - $Seep_{day}$ - Tloss

where *Waterloss* is the net movement of water out of the HRU, $Pcp_{day}$ is the precipitation, $Irr_{day}$ is the irrigation water application, $Surf_{day}$ is the surface runoff loading to the main channel, $Lat_{day}$ is the lateral flow, $GWQ_{day}$ is the groundwater contribution to streamflow, $Rvap_{day}$ is the amount of water moving from shallow aquifer to the soil profile or absorbed by plant roots in the shallow aquifer, $Rchrg_{day}$ is the amount of water recharging both aquifers, $Seep_{day}$ is the seepage leaving the bottom of the soil profile and *Tloss* are the transmission losses in surface runoff, all computed at the scale of an HRU for a particular day.

## 2.2 *Study Area: Punpun River Basin*

The study area (Figure 1) chosen was the Punpun river basin, in southern Bihar (India). The modeled area of the basin was 5495.51 km$^2$ and the outlet was chosen as the Central Water Commission gauging site at Sripalpur (25°30′06″N, 85°08′ ″E) in Patna district. The choice of the area was in part due to the fact that its land use is majorly agricultural (~74%) which is convenient for land use representation in the model.

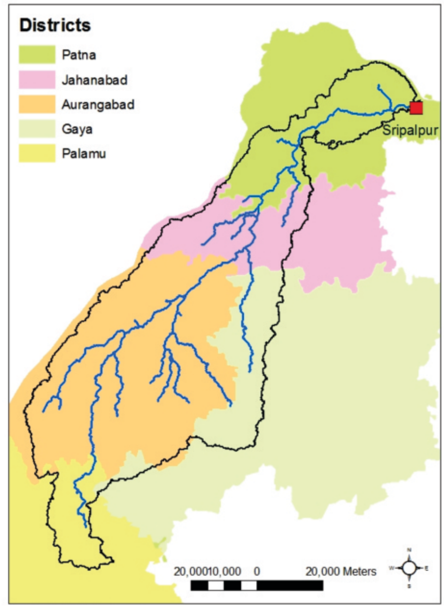


**Figure 1:** District map of the Punpun river basin

## 2.3 *Model Setup*

The input datasets required to run the SWAT model include topographical data, land use land cover (LULC) data, soil data, weather data (daily precipitation, temperature, RH, solar radiation and wind speed) and observed discharge data (output) for model calibration. Following the SWAT modeling guidelines proposed by Abbaspour et al. (2015), various combinations of input datasets were tested in multiple model runs without calibration and the combination with the best output variable simulation was chosen for calibration and further analyses. Topographic data were available from the Shuttle Radar Topography Mission (SRTM) in the form of a Digital Elevation Model (DEM) raster file. The LULC raster file was obtained from the National remote Sensing Centre (NRSC), Indian Space Research Organization (ISRO). The soil data were based on the raster dataset prepared by the NRSC and National Bureau of Soil Survey (NBSS). Most (81%) of the area had Hydrologic Group C/D soils. Daily precipitation data were derived from the Asian Precipitation Highly Resolved Observational Data Integration Towards Evaluation (APHRODITE) of Water Resources database, with a 0.5° × 0.5° resolution. The daily maximum and minimum temperature and wind speed data were extracted from the Princeton University weather dataset. The daily solar radiation and relative humidity data were derived from the National Centers for Environmental Prediction (NCEP) Climate Forecast System Reanalysis (CFSR) dataset. Daily observed discharge data ($m^3/s$) were available for the CWC gauge station at Sripalpur from 1959.

**Table 1** LULC data for Punpun basin (NRSC, ISRO)

| Sl. No. | LULC class | Area ($km^2$) | Fraction of total area (%) |
|---|---|---|---|
| 1 | *Kharif* Surface Irrigation | 1472.74 | 26.80% |
| 2 | *Kharif* Conjunctive Irrigation | 1423.25 | 25.90% |
| 3 | Current fallow | 767.90 | 13.97% |
| 4 | Double/Triple Crop Surface Irrigation | 555.33 | 10.11% |
| 5 | Double/Triple Crop Conjunctive Irrigation | 300.91 | 5.48% |
| 6 | Forest-Deciduous | 227.98 | 4.15% |
| 7 | Others (range grasses, mixed forests, *zaid* cropping) | 746.81 | 13.59% |

### 2.4 *One-at-a-time Sensitivity Analysis and Calibration/Validation*

According to the calibration protocol laid out by Abbaspour et al. (2015), the default model was used to calibrate the outlet discharge. A set of parameters expected to significantly influence the simulated discharge towards the observations was chosen out of the 26 SWAT hydrological parameters (van Griensven et al. 2006). One-at-a-time (OAT) sensitivity analysis was carried out with each of those parameters using the Latin Hypercube (LH) sampling technique. Subsequently 4 parameters (Table 2) of significance were identified, initial ranges were assigned to them and 300 simulations were run using the SWAT-CUP Sequential Uncertainty FItting Algorithm (SUFI2). The study used the Nash-Sutcliffe (NS) efficiency criterion in the objective function.

**Table 2** Model parameters used for calibration after LH-OAT sensitivity analysis

| Sl. No. | Model Parameter | Definition | Process |
|---|---|---|---|
| 1 | CN2 | SCS runoff curve number for moisture condition II | Runoff |
| 2 | ESCO | Soil evaporation compensation factor | Evaporation |
| 3 | REVAPMN | Threshold depth of water in the shallow aquifer required for return flow to occur (mm) | Groundwater |
| 4 | SOL_AWC | Available water capacity of the soil layer (mm/mm soil) | Soil |

### 2.5 *Simulation of invasion by Parthenium Hysterophorus weed at HRU-scale*

The 'Land Use Split' feature of the ArcSWAT GIS interface of SWAT was instrumental in 'splitting' the chosen LUs so that a part (50%) of the chosen HRU could be 'invaded' by *Parthenium* and then its outputs could be compared conveniently to the original LU. The choice of LUs for*Parthenium* invasion was based on a tradeoff between simulating invasions, which were most representative of actual conditions on the field, and increasing the complexity of the model by adding more details regarding phenology and weed management operations. Two criteria were used to select the LUs to be 'invaded': to choose the LU with the maximum ease of invasion for the weed, and the LU with the highest impact potential on agricultural productivity. These criteria led to two categories of LU changes or 'invasions' (Table 3) – fallow land during the dry season (January-May) and *kharif* crop LUs during the monsoon.*Kharif* crop LU management operations were incorporated from Kaur et al. (2003).Weed management was not incorporated as it would preclude the quantification of the full extent of hydrological impacts of an invasion.

**Table 3** HRU-scale *Parthenium Hysterophorus* invasion using the LU-Split feature

| Sl. No. | Original LU | Distribution of new LU | Growing season, Additional LU management inputs |
|---|---|---|---|
| 1 | Fallow Land | Fallow Land: 50%<br>*Parthenium*: 50% | January – March<br>No additional management input for both LUs |
| 2 | *Kharif* season conjunctive use \| surface irrigation | *Kharif* season conjunctive use: 50%<br>*Parthenium*: 50% | 25$^{th}$ June – 25$^{th}$ September<br>*Kharif*: 2 irrigations (120 mm each, 30% irrigation efficiency, auto-fertilization)<br>*Parthenium*: No management inputs |

## 3. Results

### 3.1 *Calibration/Validation of Outlet Discharge*

The default model (without *Parthenium* 'invasions') was run for 8 years (1990-1997) with a two year warm-up period. Observed and simulated streamflows at the outlet are given in Figure 2.

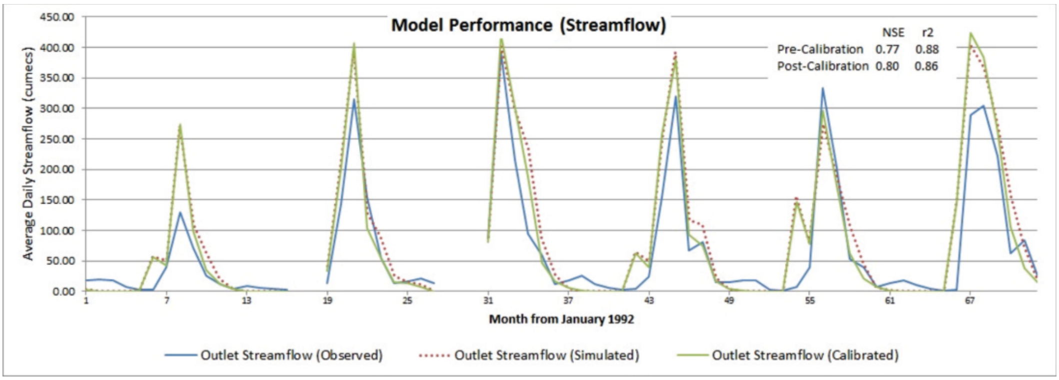


**Figure 2:** Observed, simulated and calibrated streamflows at basin outlet (Sripalpur): 1992-1997

It was observed that the peaks flows in the monsoonal wet season were consistently over-estimated by SWAT, whereas the baseflows during the dry season (January-May) were highly underestimated. According to Abbaspour et al. (2015), the over-estimation of the peak flows could be resolved by decreasing the curve number (CN2), increasing the available soil water capacity (SOL_AWC) and increasing the soil evaporation compensation factor (ESCO). Also the low base flows could be resolved by decreasing the minimum threshold for groundwater flow to occur (GWQMN), decreasing the groundwater 'revap' coefficient GW_REVAP ('revap' is the movement of water from shallow aquifer to soil profile through evaporation or root uptake by deep rooted trees) and increasing the minimum threshold of shallow aquifer for 'revap' to take place (REVAPMN). Since GWQMN=0, and GW_REVAP=0.02 were by default the minimum values that are allowed by SWAT, after LH-OAT sensitivity analysis, the other 4 parameters were chosen for calibration. Model calibration led to slightly better estimates of middle flows, but peak flows and low flows were not significantly improved. Simulated streamflow after calibration is given in Figure 2.

### 3.2 *HRU-scale Water Balance*

The average annual HRU-scale water balances were examined by equating (1) and (2) using the variables given in Table 4. SWAT computes the HRU water balance at the daily scale, so there were a few minor discrepancies when the values were aggregated to the annual level. This was resolved by the assumption that at an annual scale, the changes in the storage terms (Equation 1) were negligible. Equation 2 was used to compute an annual 'water loss/flow' balance.

**Table 4** HRU-scale Annual Water Balance (units in mm)

| PCP | IRR | ET | RCHRG | SEEP | SURQ | LATQ | GWQ | $H_2O$ Losses\|Flows |
|---|---|---|---|---|---|---|---|---|
| 936.98 | 144.42 | 586.03 | 243.29 | 240.65 | 277.18 | 2.52 | 231.00 | -1.35% |

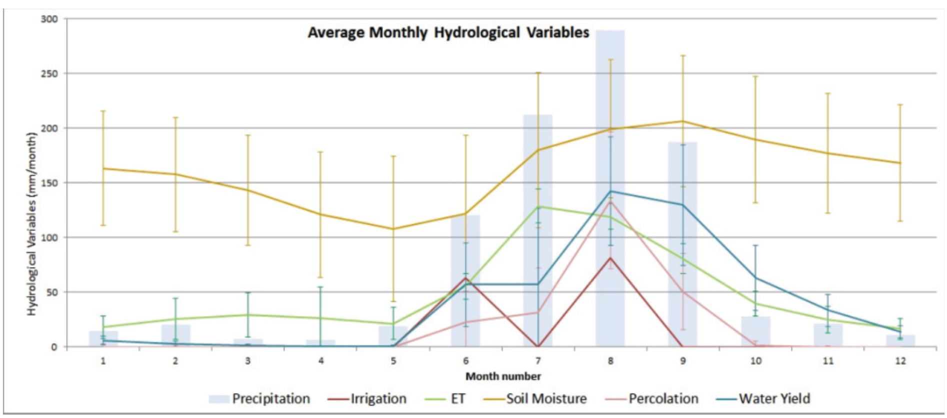


**Figure 3:** Mean monthly hydrological variables with standard deviation for relevant HRUs

A subsequent analysis was conducted on the LUs of relevance (fallow land, *kharif* crop, and *Parthenium*) by varying the soil type and slope class, independently, to understand how this variation influenced the water balance. The influence of the slope class variation on hydrological output variables while keeping other HRU components constant was negligible. This was because even despite the classification, most of the HRUs had slopes around 1% and computations did not yield large differences at this level. However, the classification of HRUs according to soil type, keeping other components constant, did yield significant differences in hydrological variables. The soil types were categorized according to Soil Hydrologic Group. The soil groups ranged from Group A to Group D. The single Group A soil had a high infiltration rate with lowest runoff potential, whereas the infiltration rates decreased simultaneously with increasing runoff potential moving towards Group D. For the sake of clarity, only the extreme soil groups A and D were chosen to compare relevant hydrological flow variables. The comparison is illustrated in Figure 4. The other groups were intermediate in their hydrological response and had variables between those of the extreme soil groups.

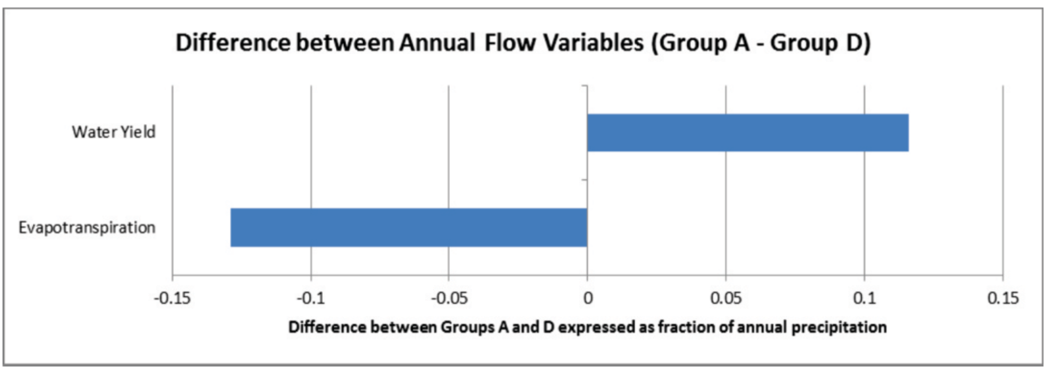


**Figure 4:** Difference of annual flow variables between Group A and Group D soils

The lower infiltration potential of Group D as compared to Group A led to a significantly higher amount of soil moisture storage in Group D which was contrasted slightly by higher aquifer storage in Group A due to higher infiltration potential. Within the water flows, Group D had significantly higher ET losses contrasted by higher surface runoff, lateral flow and base flow (Water Yield) in Group A.

3.4 HRU-scale analysis of Water Balance after Parthenium Invasion

The average monthly hydrological variables of Parthenium LU were compared to the 2 invaded LUs. Subsequently, hydrological responses of HRUs to the simulated invasions were analysed while varying the soil hydrologic groups. The Parthenium invasion is essentially a change in the SWAT crop parameters, and therefore only ET and soil moisture components of the water balance get affected. The chosen SWAT method for computing ET was the Penman-Monteith equation (Monteith J.L. 1965) which is a function of temperature, relative humidity, wind speed, solar radiation and crop parameters related to plant height, leaf area index (LAI), and stomatal conductance.

ET losses and monthly soil moisture (SW_avg) simulations averaged over all soil types and slope classes for Parthenium invasions on fallow land and kharif LU are given in Figures 5(a) and 5(b), respectively. The LAI of the crop/weed/fallow land during the growing periods, which are different for the two scenarios, are also indicated. The significant results inferred from the graphs are:

1. In the Fallow-Parthenium scenario, the ET losses are slightly higher for the weed during the first 4 months of the year, accompanied by slightly lower average soil moisture levels. Soil moisture levels are consistently lower for the weed LU. However, despite soil moisture levels decreasing for both the native and invasive LU during the dry season, the difference in ET losses leads to a relative buildup of soil moisture in the Fallow LU compared to the weed LU, and there is a short pre-monsoon period of slightly higher ET losses of Fallow LU as compared to Parthenium LU.

. For the Kharif-Parthenium scenario, ET losses of Parthenium are consistently slightly higher than for the Kharif crop LU. This is accompanied by slightly lower average soil moisture levels for the weed throughout the growing season.

3. The observed differences between ET and soil moisture are statistically insignificant at $\alpha$=0.05 for both the full year (p-value = 0.98 and 0.89 for Fallow-Parthenium ET and soil moisture, respectively; and p-value = 0.91 and 0.78 for Kharif-Parthenium ET and soil moisture, respectively) and also for only the growing season with non-zero LAI values (p-value = 0.95 and 0.86for Fallow-Parthenium ET and soil moisture; and p-value = 0.84 and 0.72 Kharif-Parthenium ET and soil moisture, respectively).

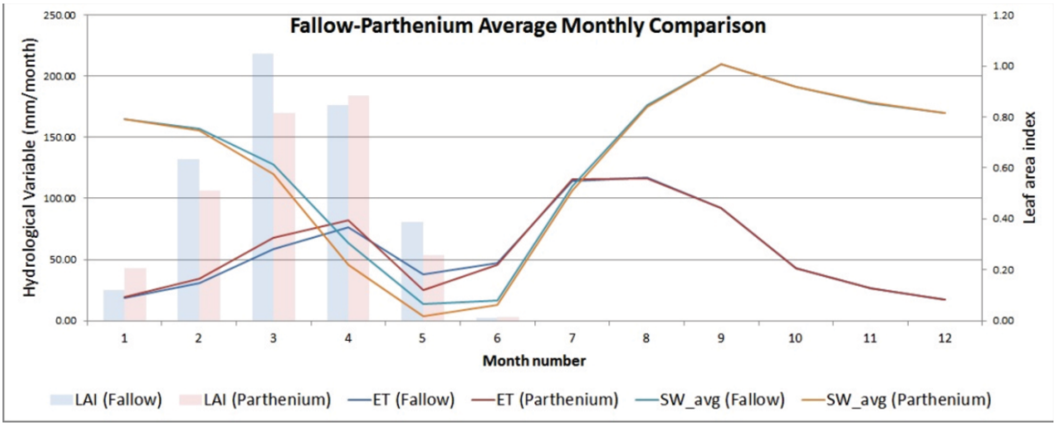


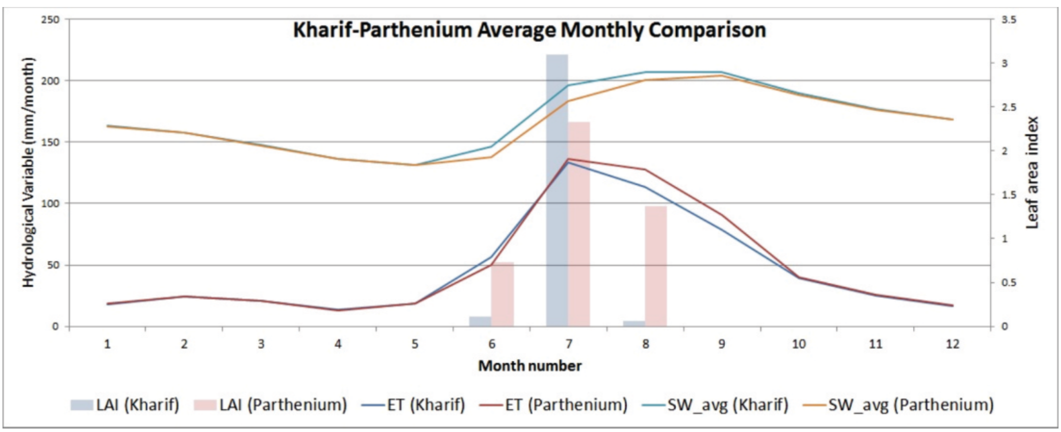


**Figure 5:** Comparison of variables for (a) Fallow-*Parthenium* and (b) *Kharif-Parthenium* simulations

These results can be explained by analyzing the SWAT crop parameters for the relevant LU types (Table 5). Higher stomatal conductance, maximum canopy height and maximum LAI (favourable leaf area development curve) lead to higher ET losses in the Penman-Monteith potential evapotranspiration (PET) calculations. This coupled with available soil moisture (which may be a limiting factor for ET in dry conditions as seen in the dry months of the Fallow-*Parthenium* scenario) can explain the modeled results satisfactorily.

**Table 5** SWAT Crop Parameters

| | Maximum LAI | Maximum stomatal conductance (s/m) | Maximum canopy height (m) |
|---|---|---|---|
| Fallow Land | 2.5 | 0.005 | 1 |
| *Kharif* season crop | 4 | 0.006 | 0.9 |
| *Parthenium* | 3 | 0.007 | 1.7 (Pandey et al. 2003) |

The same analysis when conducted by varying the soil type conserves the patterns of ET and soil moisture, but changes the amount of average monthly soil moisture. The average monthly soil moisture increases from Group A to Group D, as expected, however none of the changes were statistically significant

## 4. Discussion and Conclusion

The SWAT model simulation of *Parthenium* invasions on fallow land and native *kharif* crops using the SWAT crop parameters results in the inference that *Parthenium hysterophorus* weed has slightly higher but statistically insignificant ET losses as compared to both the native LUs. Additionally, the other objective of this HRU-scale analysis is that these ET losses follow the same trends across hydrologic soil types, which differ only in the amount of average soil water buildup in the soil layers. However, this is in conflict to the heuristic knowledge of local experts who maintain that *Parthenium hysterophorus* is a weed known for its less water uptake, and hence lesser ET losses. This discrepancy may be due to non-localized measurements of SWAT crop parameters. One example of this is the crop parameter 'Maximum Canopy Height' for *Parthenium* which was modified from 1m (SWAT estimate) to 1.7m (Pandey et al. 2003) as it was simply visible that unregulated *Parthenium* plants often grew even taller than 2m on fields and fallow land. Such regional differences may exist in other crop parameters of the relevant LUs thus requiring calibration of parameters for the local conditions of the study area.

## References


1. Abbaspour, K. C. (2007). SWAT calibration and uncertainty programs. A user manual, EAWAG: Swiss Federal Institute of Aquatic Science and Technology, 103.
2. Adla S. & Tripathi S. The Effect of *Parthenium Hysterophorus* weed on Basin Hydrology (2014). In

Tiwari H.L., Suresh S., Jaiswal R.K. *Hydraulics, Water Resources, Coastal and Environmental Engineering*. Paper presented at 19th International Conference on Hydraulics, Water Resources and Environmental Engineering: HYDRO 2014 International, Maulana Azad National Institute of Technology, Bhopal (pp 531-541). New Delhi.

3. Arnold, J. G. & Fohrer, N. (2005) SWAT2000: Current Capabilities and Research Opportunities in Applied Watershed Modelling. *Hydrol. Processes*, 19(3), 563–572.
4. Arnold, J. G., R. Srinivasan, R. S. Muttiah, and J. R. Williams. (1998). Large-area hydrologic modeling and assessment: Part I. Model development. *J. American Water Resour. Assoc*. 34(1): 73-89.
5. Dwivedi, P., Vivekanand, V., Ganguly, R., and Singh, R. P. (2009). *Parthenium* sp. as a plant biomass for the production of alkalitolerant xylanase from mutant Penicillium oxalicum SAUE-3.510 in submerged fermentation. *Biomass Energy*, 33, 581-588.
6. Gassman, P. W., Reyes, M. R., Green, C. H. & Arnold, J. G. (2007) The Soil and Water Assessment Tool: Historical Development, Applications, and Future Research Directions. *Trans. Am. Soc. Agric. Biol. Engrs*, 50(4), 1211–1250.
7. K.C. Abbaspour, E. Rouholahnejad, S. Vaghefi, R. Srinivasan, H. Yang, B. Kløve (2015). A continental-scale hydrology and water quality model for Europe: Calibration and uncertainty of a high-resolution large-scale SWAT model. *Journal of Hydrology*, 524, 733-752.
8. Kaur, R., Srinivasan, R., Mishra, K., Dutta, D., Prasad, D., & Bansal, G. (2003). Assessment of a SWAT model for soil and water management in India. *Land Use and Water Resources Research*, 3, 1-7.
9. Monteith, J. L. (1965). "Evaporation and Environment." Symposia of the Society for Experimental Biology, 19.
10. Pandey, D. K., Palni, L. M. S., and Joshi, S. C. (2003). "Growth, Reproduction and Photosynthesis of Ragweed Parthenium (*Parthenium Hysterophorus*)." *Weed Science*, 51(2), 191-201.

11. Patel, S. (2011). Harmful and beneficial aspects of *Parthenium Hysterophorus*: an update. *3 Biotech*, 1(1), 1–9. doi:10.1007/s13205-011-0007-7
12. van Griensven, A., Meixner, T., Grunwald, S., Bishop, T., Diluzio, M., & Srinivasan, R. (2006). A global sensitivity analysis tool for the parameters of multi-variable catchment models. *Journal of hydrology*, 324(1)

# ASSIMILATION OF REMOTE SENSING DERIVED SOIL MOISTURE IN MACROSCALE HYDROLOGICAL MODEL

**Vikrant Vijay Nikam [1], B R Nikam [2], Vaibhav Garg [3], S P Aggarwal [4]**

[1] Student, [2, 3, 4] Scientist/Engineer Water Resources Department,
Indian Institute of Remote Sensing, 4 Kalidas Road, Dehradun,
Uttarakhand.

***Abstract***

*This paper describes the importance of data assimilation in hydrologic model to improve the model prediction (Analysis) by merging the strength of model forecast with the satellite observations. Soil moisture is a very important variable for both the water and energy balance modes of the Land Surface Models (LSM). It is an important geophysical parameter in research on climate, hydrology, agriculture, and forestry. Soil moisture has important climatic effects by influencing ground evapotranspiration, runoff, surface reflectivity, surface emissivity, surface sensible heat and latent heat flux. At the terrestrial scale, its influence is even greater than that of sea surface temperatures; hence this crucial variable has been chosen for the assimilation in present study. The updating method uses Ensemble Kalman Filter (EnKF) concepts and involves an iterative similarity approach that avoids calculation of the Jacobian that relates the states and the observations. An EnKF data assimilation technique is applied in this study to assimilate soil moisture products derived from passive microwave remote sensing observation of Advanced Microwave Scanning Radiometer – Earth Observing System (AMSR-E), onboard Auqa. The satellite observed soil moisture data is being assimilated into the semi-distributed macroscale Variable Infiltration Capacity (VIC) model at 0.25° spatial resolution over entire Ganga basin. Four seasons have been chosen in this study from November 2004 up to October 2005 to create ensembles for selected grids from total grids. The grids are selected on the basis of maximum percentage of Land Use Land Cover (LULC) covered in particular grid and the availability of AMSR-E* *data. The assimilation has been done for ten days intervals for the selected tenure. The model was run in water balance mode at domain scale and the water budget components are updated from the EnKF so as to assure closure. It is observed that how the multilayer soil moisture regime is behaving after the data assimilation in VIC. It is reckoned that assimilation improves the soil moisture redistribution after propagating the surface soil moisture updates for entire domain compared to the model integrations without assimilation. Analysis is generated for the calculated Kalman gain matrix and it is compared with rainfall events in which assimilated soil moisture behaviour is better than that of the forecasted. This research shows that not only rainfall effect but also irrigation effect has been represented in assimilated soil moisture model. The results of water balance study for assimilated case draws attention towards the importance of data assimilation in the physical based hydrological models or LSMs.*

***Keywords:*** *Data Assimilation, soil moisture AMSR-E, VIC, EnKF.*

## Introduction

Seasonal to interannual climate predictions require two important initializing parameters such as soil moisture and sea surface temperature. Soil moisture has great influence on Land Surface Models as it controls the water and energy fluxes transfers between land and the atmosphere (Seneviratne et al. 2006; Schar et al. 1999). Today in many hydrological research the central question is analyzing and evaluating the distribution of water cycle in different forms like rainfall, runoff, infiltration, etc. in the land-atmosphere interactions (Roads et al. 2003; Pan and Wood 2005). These hydrologic cycles are influenced by the soil moisture as it controls the distribution of rainfall into runoff, baseflow, infiltration and the evaporation; influencing the surface energy fluxes (Delworth and Manabe 1988; Vinnikov and Yeserkepova 1991; Prigent et al. 2005; Sahoo et al. 2013). It is one of the factor to help in the photosynthesis of crops. It plays an important role in the growth and enhancing the various functions of the crops. Hence soil moisture plays a key role (Pielke 2001; Fang and Lakshmi

2014; Sahoo et al. 2013) in various fields like agriculture, hydrology, climate and environment (Zhang and Anthes 1982; Houser et al. 1998). Therefore an accurate quantification of the soil moisture has become very important in hydrology and climate change studies.

Yet quantifying soil moisture and analyzing its impacts on the macroscale variability in spatial and temporal domain separately with model or satellite observations or ground data alone is very difficult (Reichle et al. 2004). Hence one technique to nullify these uncertainties is to merge the remotely sense observations into the models (i.e. Data Assimilation). Remote sensing soil moisture observations can also minimize these uncertainties (Crow and Ryu 2009; Crow et al. 2005; Gao et al. 2007; Zhang et al. 2013). The current study focuses on the assimilation of remotely sensed observations into the macroscale Land Surface Model for soil moisture estimates to overcome the model forecast errors and progressively improve the model predictions. It is interested to note that there are no satellite systems existing that could give the reliable soil moisture measurements (Jackson et al. 1996).

Active/ passive remote sensors working in different microwave bands on-board satellites have been obtaining soil moisture observations and widely used in hydrology applications (Dobson and Ulaby 1986; Ulaby et al. 1996; Njoku and Entekhabi 1996; Mattikalli et al. 1998; Njoku and Li 1999; Jackson et al. 1999; Jackson et al. 2002; Schmugge 1998; Schmugge et al. 2002; Narayan et al. 2004; Lakshmi et al. 2011; Minet et al. 2012). These sensors include AMSR-E that produced C-band microwave soil moisture products at 25 km resolution (Jackson, 1993; Jackson et al., 2010; Njoku et al., 2003); SMOS (Soil Moisture and Ocean Salinity) – the first satellite sensor to provide L-band radiometer observations and 0–5 cm layer soil moisture retrievals at 40 km spatial resolution at a 3-day temporal repeat. A special issue highlighting the SMOS data calibration and validation has been published recently (Kerr et al., 2012). SMAP (Soil Moisture Active/Passive), which is the first mission to provide L-band radar and radiometer observations was launched on 31 January 2015. (Njoku and Entekhabi, 1996; Schmugge et al., 2002; Entekhabi et al., 2010; Lakshmi, 2013).

There are several data assimilation

techniques which have been used over the past few years. Sequential data assimilation techniques have been applied to various land and atmosphere parameters such as soil moisture, soil temperature, snow, oceanography and other hydrologic variables (Crow and Van Loon 2006; Pan et al. 2009; Liu et al. 2011; Andreadis and Lettenmaier 2006; Clark et al. 2006; De Lannoy et al. 2012; Bertino et al. 2003). Limited studies have been done in 1-D and 3-D variational data assimilation methods (Sahoo et al. 2013). In recent years Ensemble Kalman Filter (EnKF) which is the Monte Carlo implementation of the traditional Kalman filter (Evensen 1994) is a widely accepted data assimilation technique. It is very robust, easy to implement and the computational effi cient data assimilation scheme (Keppene 2000).

The primary objective of this study is to evaluate the performance of EnKF technique for assimilating remotely sensed surface soil moisture observations into the macroscale semi-distributed Variable Infiltration Capacity (VIC) (Liang et al. 1994) model. Hence, the goal is not necessarily to improve estimates of actual soil moisture; rather, the interest is to use soil moisture observations to update the model soil moisture initial conditions. The AMSR-E soil moisture daily product has been used in present study. Specifically, the study is based on the following questions: (a) How does the EnKF algorithm performs to assimilate AMSR-E soil moisture into the VIC? (b) What is the impact of assimilated soil moisture on the other water budget components of the VIC? (c) What is the effect of assimilation on the multi soil moisture layers regime? (d) How soil moisture is spatially varying and what is its trend after the assimilation of observations in the VIC?

In the next section, description of the study area has been given along with observations used and the essential characteristics of the VIC model. The details of the experimental setup and the algorithm of EnKF has also been given in the paper, flowed by information regarding ensemble formation for the entire Ganga basin which encompasses approximately 10, 86,000 km$^2$ area. The paper finally concludes with the results and discussions.

## 2 Description of Study Area, Observations and Land Surface Model

### 2.1 *Study Area*

The Ganga Basin, largest basin of India has been selected as study area for present study. The parts of the countries of India, Tibet, Nepal and Bangladesh together comprises of Ganga basin. The total area of Ganga basin is about 10, 86,000 $km^2$ out of which majority of geographical area is in India (i.e. basin 8, 61,452 $km^2$), which is almost slightly greater than one-fourth (26.3%) of the total geographical area of the India. Ganga basin outspreads through Bihar, Chhattisgarh, Delhi, Haryana Himachal Pradesh, Jharkhand, Madhya Pradesh, Rajasthan, Uttar Pradesh, Uttarakhand and West Bengal, in India. The basin lies between longitudes 73°2' to 89°5'E and latitudes 21°6' to 31°21'N having length of 1,543 km and width of 1024 km. The geographical extent of the Ganga basin is shown in Figure 1 which is Shuttle Radar Topography Mission (SRTM) Digital Elevation Model (DEM) of Ganga basin.

Topography of Ganga basin is very complex as the ridge of basin is formed by the Brahmaputra Ridge lies towards the east followed by the Vindhyas and Chottanagpur plateau in south while west side falls the Aravalli and towards north lies the Himalayas. The great desert of Thar and the Aravalli hills form the ridge between the Indus and Ganga drainage system. Sundarbans is amongst the largest delta of the world located in the Ganga basin. The Ganga rises in the Gangotri glacier in the Himalayas at an elevation of about 7010 m (above MSL) in the Uttarkashi district of Uttarakhand. The total length of river Ganga up to its outfall into Bay of Bengal is around 2525 km.

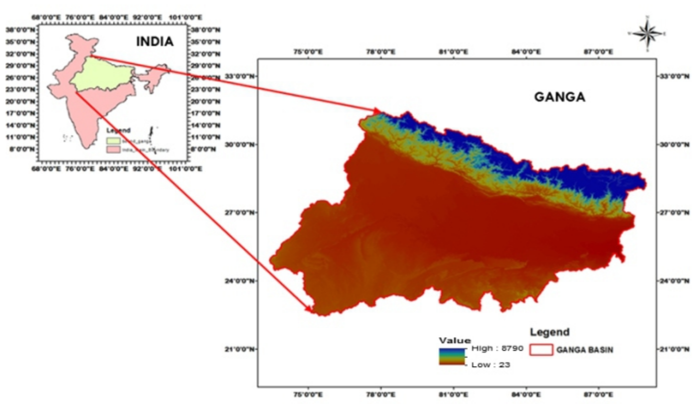


**Figure 1** Extent of the study area (Ganga Basin)

The annual average rainfall in the basin varies between 39 cm to 200 cm, with an average of 110 cm. Eighty percent of the rainfall occurs during the monsoon months i.e. from June to October. Because of large temporal variations in precipitation over the year, there is wide fluctuation in the flow characteristics of the river. On an average, each square km of the Ganga basin receives a million cubic meter (MCM) of water as rainfall. 30% of this is lost as evaporation, 20% seeps to the subsurface and the remaining 50% is available as surface runoff. The major water resources projects in Ganga are 30 which encompasses 14895.11 Th ha total culturable command area out of which 14059.56 Th ha is ultimate irrigation potential area i.e. 94.3% of culturable command area (Ganga Basin report, 2014). Therefore, soil moisture regime of the basin can't be assumed to the natural regime, however all the hydrological models assume the soil moisture in the basin as a natural regime; hence in present study soil moisture has been chosen as variable for data assimilation in hydrological model setup for Ganga basin.

### 2.2 *Observations used for Soil Moisture Data Assimilation*

The soil moisture data products derived from Advanced Microwave Scanning Radiometer-EOS (AMSR-E) sensor (Aqua platform) have been used in present study for assimilation in hydrological model. There are three standard surface soil moisture products from AMSR-E. The brightness temperature ($T_B$) observations are used for AMSR-E soil moisture datasets. All these datasets are available form 19 June 2002 at a spatial coverage of approximately 40 km are re-sampled to a global cylindrical 25 km EASE-Grid cell spacing. The AMSR-E NASA soil moisture product which is used in present study is official Level 3 soil moisture product derived from H- and V-polarized AMSR-E X band (10.6 GHz) $T_B$observations (Njoku 2008). The product is available in the NSIDC website (http://nsidc.org/data/amsre). In present study AMSR-E soil moisture retrievals from ascending (1:30 P.M. local solar time) and descending (1:30 A.M. local solar time) overpasses are combined into a single time series. This combined series is a daily soil moisture product over the basin from November 2004 to October 2005 which is converted into mm measurements by using soil bulk density equations given on NSIDC website. Soil moisture products has been then converted for the 30 cm soil layer (equivalent to thickness of top soil layer in LSM) to assimilate into the LSM.

### 2.3 *The Land Surface Model*

Land Surface Model (LSM) is a state operator in hydrologic data assimilation. In this study, Variable Infiltration Capacity (VIC) model (Liang et al. 1994, 1996; Cherkauer et al. 2003) which is a part of Soil-Atmosphere-Vegetation Transfer (SAVT) scheme has been used. VIC, a semi-distributed macroscale hydrologic model has been used in past for water resources management, land-atmosphere interactions and climate change predictions as it works in both modes such as water balance and energy balance within the grid cell; and gives statistically sub-grid variations. Its distinguish features from other LSMs are subgrid variability in vegetation classes, soil moisture storage capacity, orographic precipitation, and baseflow as a nonlinear function of the lower layer soil moisture (Gao et al. 2010; Aggarwal et al. 2013; Andreadis et al. 2006). Grid based VIC model has been used extensively in a number of macroscale river basins studies globally (Abdulla et al. 1996; Shi et al. 2008; Wood et al. 1997; Zhu and Lettenmier 2007) because of its important characteristics like vegetation heterogeneity, multiple soil layers with variable infiltration. Moisture and energy fluxes are reckoned separately for each grid associated with different vegetation classes and the elevation bands. Flow routing is then done according to the model of Lohmann et al. (1996; 1998 a) as a separate model which accounts surface and sub-surface runoff computed by VIC. Recently few attempt have been made by researchers to assimilation observed data (soil moisture, evapotranspiration, runoff and snow observations) in VIC model using various data assimilation technique (Pan and Wood 2006; Andreadis et al. 2006; Han and Li 2008).

## 3 Experiment Setup

The VIC model runs in various modes, namely energy balance, water balance and routing. In the present study, the three layers VIC (VIC-3L) model was run in water balance mode, driven by precipitation, and maximum temperature, minimum temperature and wind speed at a daily time-step, for the entire Ganga basin. It has been applied to simulate the total daily run-off potential and ET for each grid cell independently. The set-up of the VIC-3L model for the entire Ganga basin has been elaborated in next section. The complete procedure which was adopted for present study has shown in Figure 2.

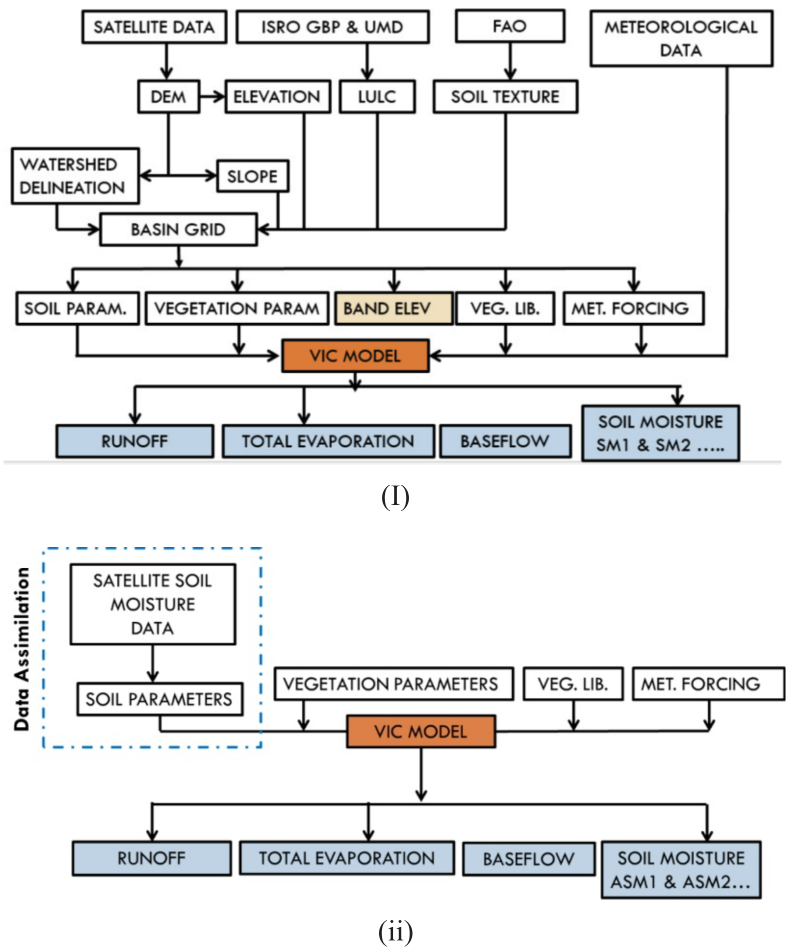


**Figure 2** Methodology adopted for the study (i) hydrologic model set up for the study area (ii) surface soil moisture assimilation done into the same model.

The attempt of data assimilation in present study begins with the simulation of VIC model in moisture budget mode that does not use any remotely sensed surface soil moisture observation i.e. Open Loop simulations. The study has been carried out for the one year from November 2004 to October 2005. The model has been calibrated for the same period and validated with the discharge data of Ganga basin at Farakka outlet which is available on the Global River Global Runoff Data Centre (GRDC) website. For discharge estimation the routing of model has been done separately by using Rout model (Lohman et al. 1996; 1998a). After calibration and validation the assimilation of AMSR-E soil moisture data has been done in the open loop simulated soil moisture through EnKF.

### 3.1 *Model implementation*

Primary focus of this study is surface soil moisture assimilation in VIC model; hence first VIC simulations were done in water balance mode to compute the soil moisture in defined number of soil layers. The three soil layers have been considered as study focused on the impact of assimilation on the multiregime soil moistures. In order to implement the VIC model, five main input files are required, namely forcing, soil parameter, vegetation parameter, vegetation library and global parameter file in ASCII format. As discussed in LSM description VIC simulates the water and energy fluxes on grid basis, the grids for entire study area have been generated first. The basin is delineated first and then grid is prepared for the entire Ganga Basin at the spatial resolution of 25 km X 25 km, using the SRTM 90 m DEM; which is further used for slope and elevation bands calculations. The total number grids generated for entire Ganga basin were 2730 out of which 1387 were the run grids.

The required inputs for VIC simulation in meteorological forcing file were daily maximum and minimum temperature, rainfall, and wind speed. The $0.25^0$ x $0.25^0$ rainfall, $1^0$ x $1^0$ daily maximum and minimum temperature, and district wise wind speed of the same resolution as that of temperature have been procured from the gridded data of Indian Meteorological Department (IMD) for the period of November 2004 to October 2005. The forcings are generated according the above mentioned data.

The soil parameter file which describes the unique soil properties for each grid cell in the model domain in addition to several other soil variables is prepared. As mentioned previously, VIC-3L has been adopted in the present analysis considering soil layers ($z1$, $z2$, $z3$) of 0–300, 300–1800 mm and 1800-2500 mm depth respectively. Hence, 03 layers of soil with 300, 1500 mm and 700 mm depth have been considered. The soil properties *viz.* soil texture, percentage sand, percentage clay and bulk density (BD) for each soil layer depth has been extracted from Food and Agriculture Organization's (FAO) soil map of the world at 1:5,000,000 scale.

The vegetation parameter file defines the number of vegetation types in each grid cell, along with their fractional coverage, root depth and its fraction. The vegetation library file defines the different land-cover types allowed in the simulation and the corresponding influencing parameters, namely architectural resistance, minimum stomatal resistance, leaf-area index, shortwave albedo, vegetation roughness length and displacement height. The vegetation parameter and vegetation library files were generated from global land cover classification map generated by the University of Maryland (UMD) at a 1 km spatial coverage.

The global parameter file is the main input file of the VIC model which sets simulation options, such as start/end dates and modes of operation, compiling the locations of the above prepared input files and directory which will store output files.

According to the above mentioned methodology the VIC model is set for the Ganga Basin and then it has been well calibrated and validated. For calibration of VIC mainly six parameters were considered *viz.* infiltration capacity ($b_i$), the maximum baseflow that can occur from the lowest soil layer ($Ds_{max}$), the fraction of $Ds_{max}$ where non-linear (rapidly increasing) baseflow begins (Ds), the fraction of the maximum soil moisture (of the lowest soil layer) where non-linear baseflow occurs (Ws) and Soil Depth (of each layer). The validation for each calibrated model has been done with the discharge data of Farakka available on GRDC website (http://www.compositerunoff.sr.unh.edu), the long term mean monthly discharge data is available on GRDC site from 1949 to 1973. For validation purpose the routing of VIC simulated runoff has been done by using Rout model. The input files required for routing were flow direction file, station location file, fraction file, unit hydrograph file in ASCII format and the fluxes simulated from VIC. All these files were given in the rout file and the channel routing were done for the entire basin. The assimilation of soil moisture has been done in VIC after the calibration and validation. Next section is about the data assimilation procedure.

### 3.2 *EnKF algorithm*

A sequential data assimilation technique – Ensemble Kalman Filter (EnKF), is applied to assimilate AMSR-E surface soil moisture in VIC. The traditional Kalman filter (KF) is the optimal sequential data assimilation method which uses Gaussian error statistics for linear dynamics and measurement processes (Gelb 1974). For nonlinear dynamics, the extended Kalman filter (EKF) can be used, although it is not stable if the nonlinearities are strong (Miller et al. 1994). Both the KF and the EKF explicitly propagate error information with a dynamic equation for the state error covariance matrix. However, the integration of this equation is not computationally feasible for large-scale environmental systems (Reichle et al. 2001). To overcome these limitations, Evensen (1994) used an ensemble of model to use nonlinear model to propagate the ensemble states. Hence in the present study EnKF has been used for assimilation scheme. The formulation of EnKF has been given below:

$$\overline{X}_i^a = \overline{X}_i^b + \hat{K}(y - H(\overline{X}_i^b)) \qquad (1)$$

$\overline{X}_i^a$ the updated estimate of the analyzed state ( n x 1 dimension and n is the number of ensembles);
$\overline{X}_i^b$ is the background model forecast, which is also referred to the first guess in data assimilation ( n x 1 dimension);
y is the observation ( p x 1 dimension and p is the number of observations), which is the soil moisture measurements in this study; H is the observation operator that converts the states in the model into observation space (p x n dimension);
$\hat{K}$ refers to the traditional Kalman gain.
The ensemble $X^b$ is given as:

$$X^b = (X_1^b, X_2^b, \dots, X_n^b \qquad (2)$$

Where we ignore time index and the subscript represents the ensemble member. The ensemble mean is then defined as

$$\overline{X^b} \quad \frac{1}{n}\sum_{i=1}^{n} X_i^b$$

The perturbation from the mean for the i th member is

$$X_i'^b = X_i^b - \overline{X^b}$$

Then $X_i^b$ is defined as a matrix formed from the ensemble of perturbations:

$$X'^b = (X'^b_1, X'^b_2, \ldots, X'^b_n) \quad (5)$$

An estimation of background error covariance is defined as

$$\bar{P}^{\bar{b}} = \frac{1}{n-1} X'^b (X'^b)^T \quad (6)$$

Then the traditional Kalman gain $\hat{K}$ can be calculated

$$\hat{K} = \hat{P}^b H^T (H\hat{P}^b H^T + R)^{-1} \quad (7)$$

R is the observation error covariance with a dimension of p x p

The procedure given above has been followed for generating assimilation parameters for the Ganga basin. The grids used for generating Kalman gain in this study are selected according to the homogeneity of land use/land cover and soil type in these girds and the availability of AMSR-E soil moisture data throughout the study period. The soil moisture assimilation has been done on ten daily basis from November 2004 to October 2005. The study period has been divided into three different seasons, as winter season (November 2004 to February 2005), summer season (March 2005 to June 2005) and monsoon season (July 2005 to October 2005).

First ensembles has been generated from the simulated soil moistures for selective hundred grids of the basin. Then ensemble perturbations were generated from the mean ensembles.

By multiplying the perturbation matrix with its transformed matrix the background error covariance has been generated. AMSR-E observations were used for the assimilation; hence the error covariance matrix has been generated by assuming 0.2 standard deviation. From generated background and error covariance matrices the Kalman gain has been calculated for the ensembles. In this study Kalman gain generation procedure has been solved through a MATLAB code developed by the authors.

The updated soil moisture i.e. assimilated soil moisture has been incorporated into the model with the help of model state file. In model state file the soil moisture for each grid with vegetation subgrid variability is calculated by the model. These subgrid variable soil moistures are given for the defined three soil depths. The MATLAB code has been developed for updating the model state files. Updated state files has been incorporated into the VIC through global parameter file end the model is run for the 10 days intervals. The VIC model provides its results in terms of flux files, each flux file contains all the water balance components solved by VIC for a particular grid. These 10 days interval fluxes then again has been appended for the complete year for each grid of Ganga basin through MATLAB code. The results from this procedure of soil moisture assimilation in VIC are discussed in following section.

## 4 Results and Discussions

Primary focus of this study is to assimilate the satellite derived soil moisture into the macroscale hydrologic model VIC. The soil moisture assimilation study has been undertaken for Nov 2004 to Oct 2005 for entire Ganga basin. AMSR-E soil moisture daily product has been assimilated and its effect on the soil moisture along with other water budget components has been observed. Both the Open Loop and assimilation simulations have been done from the files generated by the spin-up model carried out from January 1, 2000 to October 31, 2004. First VIC has been simulated in Open Loop for the year in water balance mode on daily basis for study area. Then model has been calibrated for the parameters like $b_i$, Ds, $Ds_{max}$, Ws and validated with GRDC observed discharge of Ganga; it is mean monthly discharge in cumec. For our study model is calibrated and validated for the main outlet Farakka. The calibrated and validated model simulation comparison with observed is shown in Figure 3.

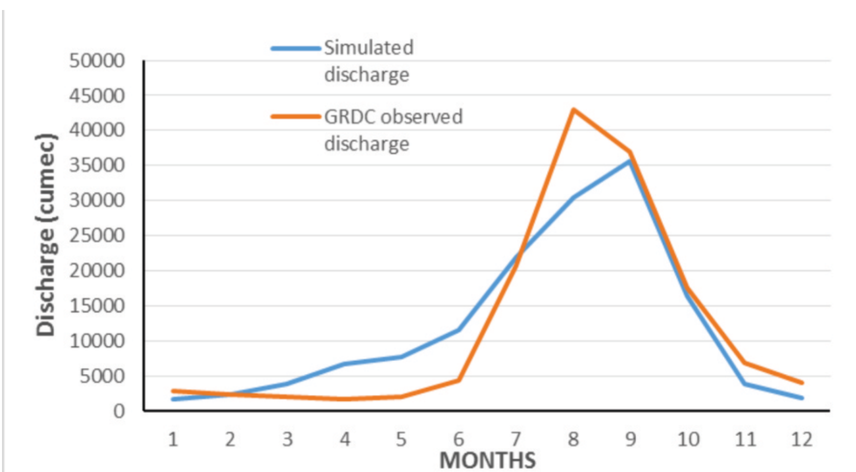


**Figure 3** Hydrograph for simulated and observed discharge of Ganga at Farakka (2004-2005)

In present study, total 47 calibration attempts have been carried out and finally the model was satisfactorily calibrated at the parameter values **$b_i$= 0.3, Ds= 0.001, Ws= 0.8** The comparison of simulated discharge from VIC with the observed discharge data can hint the success of calibration phase. The mean annual GRDC observed discharge at Farakka was 12037.26 cumec whereas calibrated model simulated mean annual discharge was 12020.92 cumec that means model was calibrated very well so it can be used for further study. Coefficient of determination between simulated and observed monthly discharge is around 0.86. The snow contribution in the discharge was also accommodated in the study though the fundamental objective of the study was to perform soil moisture assimilation in VIC.

Satellite observed soil moisture has been assimilated in the same calibrated model by EnKF for the entire Ganga from November 2004 to October 2005. The effect of surface soil moisture assimilation has been observed on the first layer and second layer soil moisture of the model which is compared along with the observation soil moisture and the rainfall. It has been clearly observed that the difference between satellites observed top layer soil moisture and soil moisture of layer one in assimilated model output is less than that of the modelled (open loop) output as depicted in Figure 4.

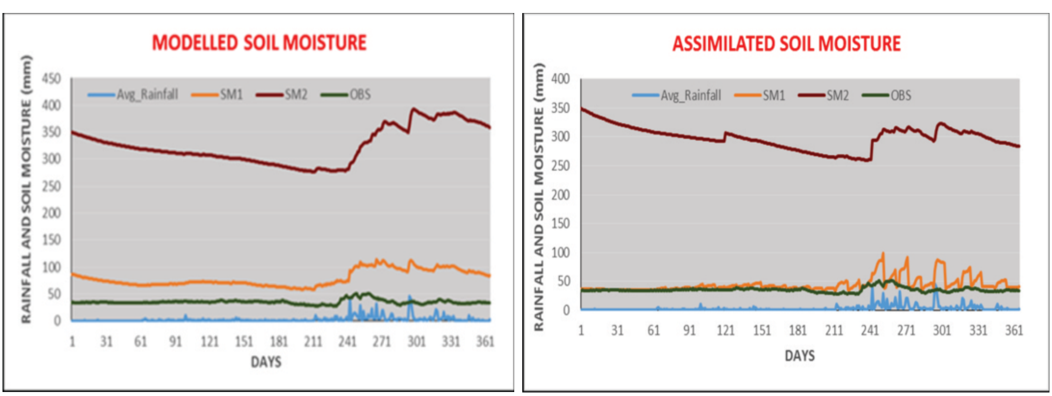


**Figure 4** Modelled Soil Moisture and Assimilated Soil Moisture for first and second soil layer comparison with rainfall and AMSR-E observed soil moisture satellite data

For first 4 to 5 days after assimilation the model behavior in terms of soil moisture was varying according to the AMSR-E observations because it has been assumed in assimilation procedure that the remotely sensed observation data is true and the standard deviation is 0.2. After approximately five days the soil moisture output of model gets slowly pulled towards the model state as the impact of observations assimilated on first day in EnKF decreases with increase in time without assimilation. In open loop simulations, soil moisture trend was govern by rainfall alone i.e. the soil moisture fluctuations have been seen only for the rainy days otherwise the soil profile varies linearly with time. In case of assimilated model output, the ups and downs can be seen in soil moisture profile of top layer, which reflect the effect of rainfall spatial dynamics and irrigation water distribution captured through satellite observed actual soil moisture on the model behavior. The impact of first layer soil moisture assimilation can be seen on the second layer soil moisture profile also. The bias between observation and surface soil moisture of open loop model has been minimized in the assimilated model.

As shown in Table 1, the relatively good impact of the assimilated soil moisture on the other water balance components have also been recorded through this study. The water balance analysis has been done for the study period and the components have been calculated for the entire year from daily average values.

**Table 1** Comparison between assimilated and modelled VIC water balance components (all units are in mm)

| | RAINFAL | RUNOF | BASEFLO | EVAPORATIO | SM1 | SM2 | SM3 |
|---|---|---|---|---|---|---|---|
| ASSIMILATED \ | 1074.62 | 239.75 | 47.15 | 423.65 | 44.20 | 298.31 | 28.04 |
| MODELLED WB | | 325.76 | 111.51 | 634.01 | 79.35 | 325.15 | 28.97 |

Open Loop simulation runoff was 325.76 mm whereas for assimilated it was 239.75mm with the difference of 86.01 mm in two approaches. The total water evaporated from the basin in Open Loop simulation was 634.01 mm whereas in assimilation model was reduced up to 423.65 mm; hence the total water contributed in baseflow was 111.51 mm and 47.15

mm respectively. The above mentioned changes in water balance components must have occurred due to reduction in top layer average soil moisture from 79.35 mm to 44.20 mm in assimilated case as compared to open loop case. It has been seen that second layer soil moisture was also changed (reduced) by 26.84 mm in assimilated approach, whereas insignificant changed has been observed in the soil moisture values of third layer in both the cases.

As the assimilation effect has been analyzed on the annual basis, the monthly effect has also been analyzed and depicted in Figure 5. It can be seen that the assimilation of satellite derived soil moisture in the top layer of VIC model has entirely changed the behavior of model in terms of water balance components.

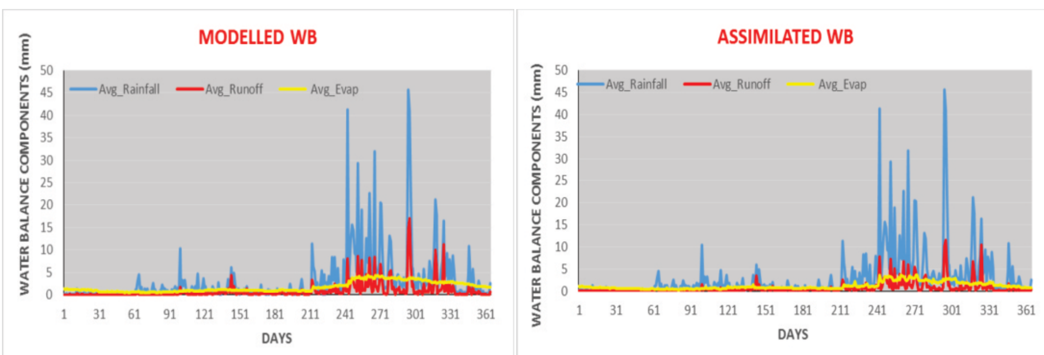


**Figure 5** Modelled Water Balance Components and Assimilated Water Balance Components

In open loop simulation water balance study, the runoff and evaporation values were more than that of the assimilated model as the soil moisture status in open loop simulation was always higher than the actual field condition (as observed through satellite). This excess water available in the top layer of soil has reduces the infiltration losses from runoff resulting in high runoff estimation in open loop case. Whereas in assimilated case the top layer soil moisture was controlled by assimilation of observations and model dynamics, hence the model tends towards the actual (observed from satellite) soil moisture condition, which is less than the open loop case. The runoff in assimilated model case is less than the open loop case due to higher deficit in soil moisture regime of the basin as discussed. The higher availability of soil moisture in open loop case has resulted in higher estimates of evapotranspiration in this case.

Previously the analysis of open loop and assimilation were made independently, study has attempted to compare the surface soil moistures of respective simulations together with their differences. As shown in Figure 6 depicts the complete scenario of the modelled soil moisture of both the cases.

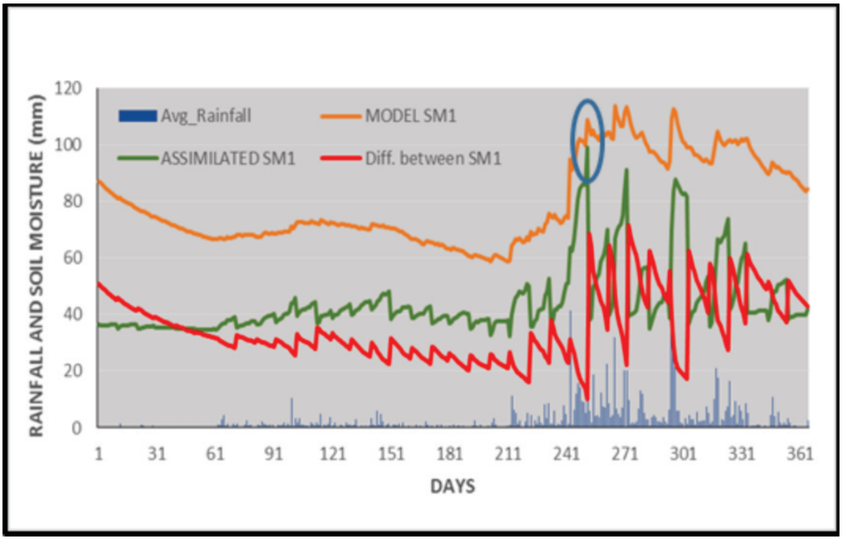


**Figure 6** First layer soil moisture comparison between modelled and assimilated VIC and difference between the same with the rainfall variations

In assimilated case the impact of rainfall spatial variations and irrigation water distribution on the soil moisture regime of the basin has successfully modeled through assimilating satellite observed soil moisture on 10 daily basis. In assimilated case, soil moisture follows rhythmic trends e.g. for first few days it is closer to the observations and then it gets pulled towards the model state as the assimilation impact became weaker and weaker with increasing time of non-assimilated period. The rounded portion in Fig.6 shows the case when the soil moisture in both the cases are almost similar, in this case very close results have been obtained from both the model setup (open loop and assimilated), the difference in runoff and the evaporation estimates of this particular day are around 0.0359 mm and 0.4615 mm respectively. It proves that the difference in water balance components in two model setups is only due to assimilation of soil moisture.

The soil moisture spatial variability has been represented in Figure 7 for the model without assimilation and model with assimilation for the 10 days interval from 21 July 205 to 31 July 2005 along with AMSR-E observations for the top most 30 cm.

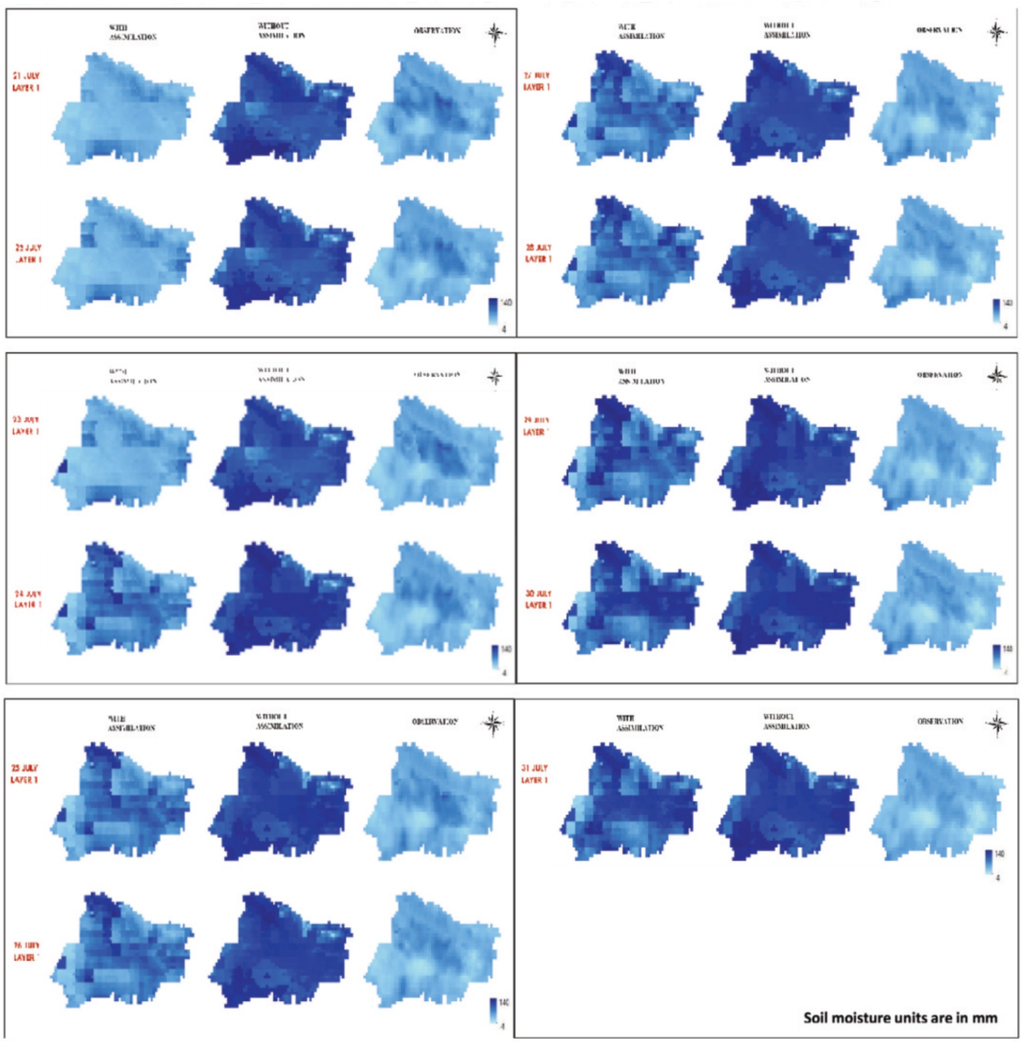


**Figure 7** Soil Moisture variability comparison for without and with assimilation VIC model for Ganga basin with AMSR-E observed soil moisture.

As discussed previously, first 4 to 5 days i.e. from 21st July to 25th or 26th July; there is a significant difference can be seen Fig. 7, between top layer soil moisture predictions of model with assimilation and without assimilation. This difference in soil moisture products of two model is governed by satellite observations of actual soil moisture which has been assimilated on the day one (i.e. 21 st July) in the model. However, the effect of actual observation assimilated model become weaker and weaker with the increase in model analysis period without assimilation, i.e. from 6th day to 10 day, this trend can be seen from 27th July to 31st July where the impact of soil moisture observations in assimilation is poor.
Similar results were obtained for each ten days intervals for the entire Ganga basin in complete study period.

**Conclusions**

This paper has investigated the performance of the Ensemble Kalman Filter (EnKF) for assimilation of remotely sensed soil moisture data in the macroscale, semi-distributed hydrological model (VIC). With high dimensions of state and parameters requirements of VIC model the optimal estimations of water balance components may be achieved, conditional to representation of actual state of study area in the model. The dynamics of actual state of basin can't be defined using any model alone. As in the most advanced LSMs also the state can be defined at the beginning of analysis only. The dynamics of basin state can only be incorporated in model through data assimilation. The primary objective of this study was to assimilated satellite derived soil moisture (which governs the water and energy balance of the basin) in the macro-scale hydrological model (VIC). The VIC model has been set up for Ganga basin at 25 km grid resolution and three level vertical discretization (i.e. soil layers). The model has been calibrated and validated using observed discharge data of Farakka. Correlation coefficient of 0.85 has been achieved during calibration and validation phase of this model. The surface soil moisture derived from passive microwave observations of AMSR-E has been assimilated in the VIC model using EnKF on ten daily basis.
The water balance study for the basin in open loop simulation (model without assimilation of satellite derived soil moisture) and assimilated case has been compared to analysis

the impact of soil moisture assimilation on the behavior of VIC model. The change in water balance components in both the cases has been observed. The modeled runoff potential of the basin decreased by 86.01 mm and the evapotranspiration losses from the basin also decreased by 210.36 mm in assimilated case. This decrease in runoff potential and evapotranspiration is attributed towards the actual soil moisture deficit of the basin, which is been incorporated in the model through assimilation.

The difference in water balance components i.e. runoff, evapotranspiration, baseflow is minimal for the time periods where the soil moisture values of top layer in open loop case and assimilated case are similar. This signifies that, the change in model behavior is governed by soil moisture assimilation. The results also indicates that, in assimilated case the model top layer soil moisture predictions are controlled by observation for first 4 to 5 days after assimilation, and further the model state plays a dominant role in governing the behavior of model. The assimilation interval in present study has been kept as 10 days, however, there are no standards available for deciding time interval between two assimilation steps, further research can be taken up for optimizing the time interval for assimilation of different variable.

The daily soil moisture update through assimilation improves the behavior of model and hence estimation of hydrological components. It is recommended that assimilation is essential for the models dealing with highly dynamic state variables. Data assimilation techniques enhances the capability of model on the cost of increased computational burden.

**References**


1. Abdulla, F. A., D. P. Lettenmaier, E. F Wood, and J. A Smith. (1996). Application of a macroscale hydrologic model to estimate the water balance of the Arkansas Red River basin. *J. Geophys. Res.-Atmos, 101 (D3),* 7449-7459.
2. Andreadis, K. and D. P. Lettenmaier. (2006). Assimilating remotely sensed snow observations into a macroscale hydrology model. *Advances in Water Resources*, *29*, 872–886.
3. Andreadis, K. M., and D.P. Lettenmaier. (2006a). Trends in 20th century drought over the continental United States.

*Geophys Res Lett, 33(10).*
4. B. Fang, V. Lakshmi. (2014). Soil moisture at watershed scale: Remote sensing techniques. *Journal of Hydrology 516* 258–272
5. Cherkauer, K. A., L. C. Bowling, D.P. Lettenmaier. (2003). Variable infiltration capacity cold land process model updates*Global Planet Change, 38(1-2),* 151-159.
6. Clark, M. P., A. G. Slater, A. P. Barrett, L. E. Hay, G. J. McCabe and B. Rajagopalan. (2006). Assimilation of snow covered area information into hydrologic and land-surface models. *Advances in Water Resources*, *29*, 1209–1221.
7. Crow, W. T. and E. Van Loon, (2006). Impact of incorrect model error assumptions on the sequential assimilation of remotely sensed soil moisture. *Journal of Hydrometeorology, 7*,421–432.
8. Crow, W., and D. Ryu (2009). A new data assimilation approach for improving runoff prediction using remotely-sensed soil moisture retrievals. *Hydrology and Earth System Sciences, 13(1),* 1.
9. Crow, W., R. Bindlish, and T. Jackson. (2005).The added value of spaceborne passive microwave soil moisture retrievals for forecasting rainfall-runoff partitioning. *Geophysical Research Letters, 32(18).*
10. De Lannoy, G. J. M., R. H. Reichle, P. R. Houser, K. Arsenault, N. E. C. Verhoest, V. R. N. Pauwels. (2012). Multiscale assimilation of Advanced Microwave Scanning Radiometer-EOS snow water equivalent and Moderate resolution Imaging Spectroradiometer snow cover fraction observations in northern Colorado. *Water Resources Research*, *48*, W01522, doi: 10.1029/2011WR010588.
11. Delworth, T. L. and S. Manabe. (1988).The influence of potential evaporation on the variabilities of simulated soil wetness and climate. *Journal of Climate*, *l*, 523-547.
12. Dobson, M.C., Ulaby. (1986). Active microwave soil moisture research. IEEE Trans. *Geosci. Remote Sens. 1,* 23–36.
13. Entekhabi, D., E.G. Njoku, P.E. O'Neill, K.H. Kellogg, W.T. Crow, W.N Edelstein. (2010).The soil moisture active passive (SMAP) mission. Proc. *IEEE 98 (5),*

704–716.

14. Evensen, G. (1994). Sequential data assimilation with a nonlinear quasi geostrophic model using Monte Carlo methods to forecast error statistics. *Journal of Geophysical Research, 99(C5),* 10,143–10,162.
15. Gao H., E. F. Wood, M. Drusch, and M. F. McCabe (2007). Copula-derived observation operators for assimilating TMI and AMSR-E retrieved soil moisture into land surface models. *Journal of Hydrometeorology, 8(3),* 413-429.
16. Gao, H., Q. Tang, X. Shi, C .Zhu, T .Bohn, F .Su, J .Sheffield, M .Pan, D. P. Lettenmaier, E. F. Wood. (2009) Water Budget Record from Variable Infiltration Capacity (VIC) Model.
17. Gelb A. (1974). Applied Optimal Estimation. *The MIT Press,* pp 374.
18. Han, X., and X. Li (2008). An evaluation of the nonlinear/non-Gaussian filters for the sequential data assimilation. *Remote Sensing of Environment,112*(4), 1434-1449.
19. Houser, P.R., W.J. Shuttleworth, J.S. Famiglietti, H.V.Gupta, K.H Syed, D.C. Goodrich. (1998). Integration of soil moisture remote sensing and hydrologic modeling using data assimilation. *Water Resour. Res. 34 (12),* 3405–3420.
20. Jackson, Thomas J. (1993). Measuring surface soil moisture using passive microwave remote sensing. *Hydrol. Process. 7 (2),* 139–152.
21. Jackson, J. Thomas, Cosh, H. Michael, Bindlish, Rajat, Starks, J. Patrick., Bosch, D. David., Seyfried, Mark, Goodrich, C. David., Moran, Mary Susan, Du, Jinyang. (2010). Validation of advanced microwave scanning radiometer soil moisture products. *IEEE Trans. Geosci. Remote Sens. 48 (12),* 4256–4272.
22. Jackson, T. J. Thomas, Le Vine, M. David, Hsu, Y Ann, Oldak, Anna, Starks, J. Patrick., Swift, T. Calvin., Isham, D. John., Haken, Michael (1999). Soil moisture mapping at regional scales using microwave radiometry: the Southern Great Plains Hydrology Experiment. *IEEE Trans. Geosci. Remote Sens. 37 (5),* 2136– 2151.
23. Keppenne C L. (2000). Data assimilation into a primitive-equation model with a parallel

ensemble Kalman filter. *Mon Weather Rev; 128* :1971–81.

24. Kerr, Y.H., J. Font, M. Martin-Neira, S. Mecklenburg, (2012). Introduction to the special issue on the ESA's Soil Moisture and Ocean Salinity Mission (SMOS): instrument performance and first results. *IEEE Trans. Geosci. Remote Sens. 50 (5),* 1351–1353.
25. Lakshmi, V. (2013). Remote sensing of soil moisture. *ISRN Soil Sci*. 2013, 33.
26. Lakshmi, Venkat, Hong, Seungbum, Small, E. Eric, Chen, Fei. (2011).The influence of the land surface on hydrometeorology and ecology: new advances from modeling and satellite remote sensing.*Hydrol. Res. 42 (2–3)*, 95–112.
27. Laurent Bertino, Geir Evensen and Hans Wackernage. (2007). Sequential Data Assimilation Techniques in Oceanography. *International Statistical Review(* 71, 2),223–241.
28. Liang, X., D. P. Lettenmaier, E. F. Wood, S. J. Burges. (1994). A simple hydrologically based model of land-surface water and energy fluxes for general-circulation models*J. Geophys. Res.-Atmos., 99(D7),* 14415-14428.
29. Liang, X., D. P. Lettenmaier, E. F. Wood, S. J. Burges. (1996). Surface soil moisture parameterization of the VIC-2L model: Evaluation and modification. *Global Planet Change, 13(1-4),* 195-206.
30. Liu Q., R. H. Reichle, R. Bindlish, M. H. Cosh, W. T. Crow, R. de Jeu, G. J. M. De Lannoy, G. J. Huffman and T. J. Jackson. (2011).The contributions of precipitation and soil moisture observations to the skill of soil moisture estimates in a land data assimilation system. *Journal of Hydrometeorology*, *12*, 750-765, doi: 10.1175/JHM-D-10-05000.
31. Lohmann, D. E. Raschke, B. Nijssen. (1996). A large scale horizontal routing model to be coupled to land surface parameterization schemes. *Tellus (48A),* 708-721.
32. Lohmann, D., E. Raschke, B. Nijssen, D.P. Lettenmaier. (1998a). Regional scale hydrology: I. Formulation of the VIC-2L model coupled to a routing model. *Hydrol. Sci. J.-J. Sci. Hydrol., 43(1),* 131-141.
33. Lohmann, D., E. Raschke, B. Nijssen, D.P. Lettenmaier.

(1998b). Regional scale hydrology: II. Application of the VIC-2L model to the Weser River, Germany. *Hydrol. Sci. J.-J. Sci. Hydrol., 43(1),* 143-158.

34. Mattikalli, N., E.T. Engman, L.R. Ahuha, T.J. Jackson. (1998). Microwave remote sensing of soil moisture for estimation of profile soil property. *Int. J. Remote Sens. 19 (9),* 1751–1767.
35. Miller, D. A. and R. A. White, (1998). A Conterminous United States Multilayer Soil Characteristics Dataset for Regional Climate and Hydrology Modeling. *Earth Interactions, 2(2),* 1-26.
36. Minet, Julien (2012). Validation of ground penetrating radar full-waveform inversion for field scale soil moisture mapping. *J. Hydrol. 424*, 112–123.
37. Ming Pan and E. F. Wood. (2005). Data Assimilation for Estimating the Terrestrial Water Budget Using a Constrained Ensemble Kalman Filter. *Journal of Hydrometeorology for the special CAHMDA issue.*
38. Narayan, U., V. Lakshmi, E.G. Njoku. (2004). Retrieval of soil moisture from passive and active L/S band sensor (PALS) observations during the Soil Moisture Experiment in 2002 (SMEX02). *Remote Sens. Environ. 92 (4),* 483–496.
39. Njoku, E.G., D. Entekhabi. (1996). Passive microwave remote sensing of soil moisture. *J. Hydrol. 184 (1),* 101–129.
39. Njoku, G. Eni (2003). Soil moisture retrieval from AMSR-E. *IEEE Trans. Geosci. Remote Sens. 41.2*, 215–229.
40. Njoku, G. Eni. Li Li. (1999). Retrieval of land surface parameters using passive microwave measurements at 6–18 GHz*IEEE Trans. Geosci. Remote Sens. 37 (1 3),* 79–93.
41. Pan, M., and E. F. Wood. (2006). Data assimilation for estimating the terrestrial water budget using a constrained ensemble Kalman filter. *Journal of Hydrometeorology, 7*(3), 534-547.
42. Pan, M., E. F. Wood, D. B. McLaughlin, D. Entekhabi and L. Luo. (2009). A multi-scale ensemble filtering system for hydrologic data assimilation: Part I, implementation and synthetic experiment. *Journal of Hydrometeorology, 10 (3),* 794–806, doi:

10.1175/2009JHM1088.1.

43. Pielke, R.A. (2001). Influence of the spatial distribution of vegetation and soils on the prediction of cumulus convective rainfall. *Rev. Geophys. 39 (2),* 151–177.

44. Prigent, C., F. Aires, W. B. Rossow and A. Robock, (2005) Sensitivity of satellite microwave and infrared observations to soil moisture at a global scale: Relationship of satellite observations to in situ soil moisture measurements. *Journal of Geophysical Research, 110*, D07110, doi: 10.1029/2004JD005087.

45. Reichle, R. H., R. D. Koster, J. Dong and A. A. Berg, (2004) Global soil moisture from satellite observations, land surface models, and ground data: Implication for data assimilation. *Journal of Hydrometeorology*,*5*, 430–442.

46. Roads, J., R. Lawford, E. Bainto, E. Berbery, S. Chen, B. Fekete, K. Gallo, A. Grundstein, W. Higgins, M. Kanamitsu, W. Krajewski1, V. Lakshmi, D. Leathers, D. Lettenmaier, L. Luo, E. Maurer, T. Meyers, D. Miller, K. Mitchell, T. Mote, R. Pinker, T. Reichler, D. Robinson, A. Robock, J. Smith, G. Srinivasan, K. Verdin, K. Vinnikov, T. Vonder Haar, C. Vorosmarty, S. Williams, E. Yarosh, (2003) GCIP Water and Energy Budget Synthesis (WEBS). *J. Geophys. Res., 108 (D16),* 10.1029/2002JD002583.

47. Sahoo, A.K., G.J.M De Lannoy, R.H Reichle, P.R. Houser. (2013) Assimilation and Downscaling of Satellite Observed Soil Moisture over the Little River Experimental Watershed in Georgia, USA. *Advances in Water Resources*.

48. Schär, C., D. Luthi, U. Beyerle and E. Heise, (1999) The soil-precipitation feedback: A process study with a regional climate model. *Journal of Climate, 12*, 722–741.

49. Schmugge, T.J., W.P Kustas, J.C Ritchie, T.J Jackson, A Rango. (2002). Remote sensing in hydrology. *Adv. Water Resour. 25 (8),* 1367–1385.

50. Schmugge, Thomas, (1998). Applications of passive microwave observations of surface soil moisture *J. Hydrol. 212,* 188–197.

51. Seneviratne, S. I., D. Luthi, M. Litschi and C. Schär, (2006): Land–atmosphere coupling and

climate change in Europe. *Nature, 443(7108)*, 205–209.

52. Shi, X. G., A. W. Wood, and D. P. Lettenmaier (2008) How Essential is Hydrologic Model Calibration to Seasonal Streamflow Forecasting? *Journal of Hydrometeorology, 9(6),* 1350-1363.
53. T. J. Jackson, J. Schmugge, E. T. Engman (1996) Remote sensing applications to hydrology: soil moisture. *Hydrological Sciences - Journal- des Sciences Hydrologiques, 4l (l)* August.
54. Ulaby, F.T., P.C Dubois, J., Van Zyl (1996). Radar mapping of surface soil moisture.*J. Hydrol. 184 (1),* 57–84
55. Vinnikov, K. Y. and I. B. Yeserkepova, (1991). Soil moisture: Empirical data and model results. *Journal of Climate*, *4*, 66-79.
56. Wood E.F., D.P. Lettenmaier, X. Liang, D. Lohmann, A. Boone, S. Chang, F. Chen, Y. Dai, R.E. Dickinson, Q. Duan, M. Ek, Y.M. Gusev, F. Habets, P. Irannejad, R. Koster, K.E. Mitchel, O.N. Nasonova, J, Noilhan, J. Schaake, A. Schlosser, Y. Shao, A.B. Shmakin, D. Verseghy, K. Warrach, P. Wetzel, Y. Xue, Z.L. Yang, Q. Zeng, (1997). The Project for Intercomparison of Land-surface Parameterization Schemes (PILPS) phase 2(c) Red-Arkansas River basin experiment: 1. Experiment description and summary Intercomparison. *Elsevier Science*.
57. Yu Zhang, Yang Hong, J.Jonathan, Gourley, Xuguang Wang, G. Robert Brakenridge, Tom De Groeve and Humberto Vergara. (2013). Impact of Assimilating Spaceborne Microwave Signals for Improving Hydrological Prediction in Ungauged Basins. *Remote Sensing of the Terrestrial Water Cycle*
58. Zhang, D., R.A Anthes, (1982). A high-resolution model of the planetary boundary layer-sensitivity tests and comparisons with SESAME-79 data*I. Appl. Meteorol. 21 (11),* 1594–1609
59. Zhu, C. M., and D. P. Lettenmaier (2007) Long-term climate and derived surface hydrology and energy flux data for Mexico: 1925-2004. *J. Clim., 20(9),* 1936-1946.

# TOTAL SEDIMENT TRANSPORT MODEL BASED ON DIMENSION LESS PARAMETERS

**Vipin Kumar Yadav [1], Dr. S. M. Yadav[2]**

[1]Student M. Tech (WRE), SVNIT, Surat.

[2]Prodessor, Civil Engineering Department, SVNIT, Surat.

***Abstract***

*Methods of sediment transport rate by using relationships suggested by various researchers are conventionally compared for finding total load in a stream, for a given set of flow parameters. Concepts of probability, empiricism, stream power, regression and power balance have been explored and tested, yet any singular relationship fails to prove accurate for prediction of sediment transport rate in any stream. This ultimately compels the practising Engineer to test a number of approaches before using any one in the field application. Alternative method suggested by some researchers is to find the best correlation between various dimensionless flow parameters and different dimensional as well as non-dimensional sediment transport parameters. The present study aims to evaluate the correlation between dimensionless sediment transport parameter and dimensionless flow parameters. A regression model is proposed for total sediment rate prediction after testing it for number of data sets from both laboratory and field. This approach lacks theoretical validation, in terms of physical processes however, the concept of non-dimensionality is scientific and relieves analysis from complexity of units and their conversions. The proposed model can be applied more freely to any set of observations. Based on this methodology, the model is developed using five data sets with 320 data points. The model has been tested on other independent data sets of Steins, Willis, Portugal River and Rio Grande (Nordin). The mean normalised error in the prediction is found to be -53.97% to 65.30%.*

**Keywords:** *Total sediment transport, dimensionless parameters, correlation coefficient*

## Introduction

Sediment transport is a key factor affecting the stability and design of various hydraulic structures across an open water channel. Immense quantities of sediment of various sizes, shapes and density get carried away by different modes of movement like bed load, suspended load and wash load, depending upon the flow and channel characteristics. The hydraulics of flow in a river and its sediment transport characteristics are the two basic phenomena that determine its geometrics and plan form shape. There are many variables that affect the hydraulics of flow and the nature of sediment transport in a natural stream. Theoretical developments of sediment transport functions for different flow and sediment conditions were based on assumptions of different degrees of complexity. Some of the simplified assumptions are based on idealized laboratory conditions that may not be true for the much more complicated natural river systems. In the present study effort is being made to study dimensionless flow parameters influencing strongly on sediment transport rate and thus predict total sediment transport rate.

## 2. Total Sediment Transport

The basic mechanism responsible for sediment motion is the drag force exerted by the fluid flow on individual grains (Henderson, 1966). The knowledge and correct prediction of total sediment load carried by the channel is necessary to tackle hydraulic problems like aggradation, degradation, river training etc. The behaviour of sediments in varying flow conditions remains impossible to predict. Its prediction has been tried from all angles considering and ignoring many parameters of flow and geometry, yet the dynamic nature of flow and innumerable combinations of sediment size and shape keep the research an open challenge.

Shu-Qing Yang (2005)23 studied the correlations between the total sediment discharges and various hydraulic parameters were examined by using field and laboratory data and obtained new transport parameter. Author found that Dou's energy parameter, V3/ghω as well as Yang's parameter VS/ω does not correlate well with selected data sets. **S.K. Sinnakaudan, M.S. Sulaiman, S.H. Teoh (2010)**[25] developed total load transport model using the multiple linear regression analysis approach based on Engelund & Hansen (1967) equation. **Jennifer G. Duan (2013)**[8] developed total sediment load model based on 4000 sets of laboratory experimental data and 3000 sets of field data and dimensionless parameters are formulated to quantify total sediment load. A simplified power-law relation is formulated from fitting the measured data.

## 3. Methodology

Based on observed data values of parameters like depth of flow, width of channel, sediment mean size, velocity of flow, slope of channel, etc. and observed sediment transport rate, the values of other significant parameters like shear stress, critical shear velocity, friction velocity and other dimensionless flow parameters like $\varphi_b$, $\varphi_v$, $\varphi_y$, $\varphi_e$, $\varphi_n$, $\varphi_d$ are calculated. The observed sediment transport rate is converted into dimensionless form using the relationship of Einstein. This dimensionless sediment transport rate is tested for correlation with each dimensionless flow parameter. The pair showing the best correlation is selected to develop a regression equation for a large number of data set values plotted for the selected pair of parameters. The developed model is tested on independent data sets to validate. The obtained result is analysed using statistical parameters like mean percentage error, discrepancy ratio and score, etc. and conclusions are drawn.

Following dimensionless flow parameters and sediment transport parameters were calculated for the analysis (given in equations 1-7:

a) $\varphi_b$ (Bagnold Power Parameter),

$\Phi_b = \tau_0 V$ (1)

b) $\varphi_v$ (Van Rijn's excessive dimensionless shear stress Parameter),

$\Phi_v = (u'^2_* - u^2_{*c}) / u^3_*$ (2)

c) $\varphi_y$ (Yang's Stress Parameter),

$\Phi_y = VS/\omega$ (3)

d) $\varphi_e$ (Dou's Energy Parameter),

$\Phi_e = V^3/g*R*\omega$ (4)

e) $\varphi_n$ (Yang and Lim Parameter),

$\Phi_n = (\Upsilon_s/\Delta\Upsilon_s)*\tau_0*(u'^2_* - u^2_{*c})/\omega$ (5)

f) $\varphi_d$ (Duan Parameter), $\Phi_d = [(u'_* - u_{*c}) *\tau_0]/[\omega*(\Delta\Upsilon_s d)]$ (6)

Sediment transport parameters

a) Einstein Dimensionless transport parameter

$q_{s1}* = q_s / [\{\Upsilon s/\Upsilon - 1\}\, g\, d^3]^{1/2}$ where $q_s$ is in $m^2/s$ (7)

## 4. Data Collection

Data collected contains laboratory experimental data and field data in canals and natural rivers. The range of lab data and field data is given in Table 1 & 2 respectively. These data sets were used for analysis, model development and testing/validation of developed model.

**Table 1** Summary of Laboratory Data used for analysis

| Ranges of Laboratory Data used in the Analysis | | | | | | | |
|---|---|---|---|---|---|---|---|
| Data Set | No. of Data Points | Q | | B | | D | |
| | | m3/s | | m | | M | |
| J P Soni | 23 | 0.0014 | 0.009 | 0.2 | 0.2 | 0.022 | 0.1 |
| Steins | 56 | 0.078152 | 0.482372 | 1.219 | 1.219 | 0.0914 | 0.3658 |
| Willis | 32 | 0.016423 | 0.048137 | 0.36 | 0.36 | 0.1036 | 0.1494 |
| Abdel Aal F M | 10 | 0.010703 | 0.03582 | 0.305 | 0.305 | 0.0914 | 0.1402 |
| Einstein H A | 16 | 0.073907 | 0.082968 | 0.307 | 0.307 | 0.1085 | 0.1423 |
| Gibbs C H | 9 | 0.15857 | 0.198212 | 1.219 | 1.219 | 0.1707 | 0.1768 |
| Nomicos (1956) | 16 | 0.00476 | 0.01571 | 0.2669 | 0.2669 | 0.068003 | 0.07381 |
| Barton and Lin | 28 | 0.025484 | 0.257675 | 1.219 | 1.219 | 0.0914 | 0.4206 |
| Williams G P | 177 | 0.001048 | 0.162336 | 0.076 | 1.189 | 0.025 | 0.311 |

| Data Set | U | | S | | d50 | | T | |
|---|---|---|---|---|---|---|---|---|
| | m/s | | | | m | | Degree C | |
| J P Soni | 0.21875 | 0.612069 | 0.00207 | 0.007 | 0.00032 | 0.00032 | 27 | 31.5 |
| Steins | 0.420679573 | 1.841582 | 0.00061 | 0.0427 | 0.000399 | 0.000399 | 20 | 28.9 |
| Willis | 0.326416778 | 1.197407 | 0.000831 | 0.00858 | 0.00054 | 0.00054 | 10.83 | 37.78 |
| Abdel Aal F M | 0.383936579 | 0.889172 | 0.0017 | 0.0025 | 0.000105 | 0.000105 | 23 | 23 |
| Einstein H A | 1.870121967 | 2.218796 | 0.0124 | 0.0258 | 0.000274 | 0.0013 | 17 | 26 |
| Gibbs C H | 0.748889087 | 0.952561 | 0.0029 | 0.005 | 0.004374 | 0.004374 | 24 | 24 |
| Nomicos (1956) | 0.242609582 | 0.800714 | 0.002 | 0.0039 | 0.000137 | 0.000152 | 25 | 26 |
| Barton and Lin | 0.226283807 | 1.093126 | 0.00044 | 0.0021 | 0.00018 | 0.00018 | 14.3 | 26.5 |
| Williams G P | 0.047167 | 6.479933 | 0.0006 | 0.0367 | 0.001349 | 0.001349 | 8.06 | 28.61 |

**Table 2** Summary of Field Data used for analysis

| Ranges of Field Data used in the Analysis | | | | | | | | |
|---|---|---|---|---|---|---|---|---|
| S.No | Data Set | No. of Data Points | Q | | B | | D | |
| | | | m3/s | | m | | M | |
| 1 | Portugal River | 219 | 26.99911 | 797.4989 | 69.601 | 188.939 | 0.4575 | 2.4414 |
| 2 | RED River-Toffaletti | 30 | 190.2834 | 1537.558 | 16.897 | 182.88 | 2.9992 | 7.3762 |
| 3 | American Canal Simons | 11 | 1.217588 | 29.42031 | 3.2 | 22.189 | 0.7955 | 2.5908 |
| 4 | Rio Grande- Nordin | 293 | 0.498361 | 285.9915 | 7.925 | 121.92 | 0.1585 | 3.1181 |

| S.No | Data Set | U | | S | | d50 | | T | |
|---|---|---|---|---|---|---|---|---|---|
| | | m/s | | | | m | | Degree C | |
| 1 | Portugal River | 0.6421 | 16.9788 | 0.00007 | 0.00099 | 0.002204 | 0.002204 | 10 | 10 |
| 2 | RED River-Toffaletti | 0.3699 | 6.2235 | 6.61E-05 | 0.000752 | 0.000094 | 0.000217 | 3 | 35 |
| 3 | American Canal Simons | 0.4152 | 0.7666 | 0.000058 | 0.00033 | 0.000096 | 0.007 | 16.67 | 26.11 |
| 4 | Rio Grande-Nordin | 0.1927 | 2.3841 | 0.00069 | 0.00246 | 0.000044 | 0.010954 | 0 | 28.89 |

## 5. Data Analysis

For the development of model for predicting total sediment transport rate calculations are done for all the data sets using MS Excel spread-sheet. The correlation coefficients were found between qs1* and dimensionless flow parameters ($\varphi_b$, $\varphi_v$, $\varphi_y$, $\varphi_e$, $\varphi_n$, $\varphi_d$). Graphs were plotted between each such correlation. Subsequently qs1* is found best correlated with $\varphi_d$ and thus $R^2$ value obtained for power relation curve fitting each data set was assessed. Further, based on this analysis a set of best data sets were selected, based on $R^2$ values from 0.35 to 0.95, for developing a model.

During the process of calculation of dependent parameters, like shear stress, friction velocity, etc. from the given parameter like D, S, etc., Zanke's formula, eq. (8), has been used for calculating fall velocity and kinematic viscosity has been calculated considering the temperature effect using equation (9).

$$\omega = [(10*\upsilon/d)\ [\{1 + (0.01\Delta_s *g * d^3/\upsilon^2)\}^{1/2} - 1]]\ \text{m/s} \qquad (8)$$

$$\upsilon = (1.792*0.000001)/((1+(0.0337*T)+(0.000221*T^2)))\ \text{m}^2\text{/s} \qquad (9)$$

Where, T is temperature in degree centigrade.

Critical Shear velocity has been found using modified Shield's curve and Guo (1997) relation (10) for field data where mean sediment size changes very frequently.

$$\frac{U_{*c}^2}{(S-1)\,g\,d_J} = 0.095 S_*^{-\frac{2}{3}} + 0.056\left[1 - \exp\left(\frac{-S_*^{\frac{3}{4}}}{20}\right)\right] \qquad (10)$$

Where,

$$\upsilon = \frac{1.792 * 0.000001}{(1 + (0.0337 * \text{Temperature}) + (0.000221 * (\text{Temperature}^2))}$$

$$d_\sigma = d_{50} \left(\frac{\Delta g}{V^2}\right)^{\frac{1}{3}}$$

$$S_* = \left[\frac{d_\sigma}{4\upsilon}\right] [(S-1) g \, d_\sigma]^{0.5}$$

Correlation coefficients for each data set between sediment transport parameter and flow parameter is found using eq. (11) as shown in sample Table 3.

Correlation Coefficient =

$$\frac{\Sigma(xi - xavg)(yi - yavg)}{\Sigma\sqrt{[(xi - xavg)^2 (yi - yavg)^2]}} \quad (11)$$

**Table 3** Sample Correlation Coefficient Table for data set of Williams G P

| | ϕn | ϕb | ϕv | ϕy | ϕe | ϕd |
|---|---|---|---|---|---|---|
| **qs1*** | 0.858763 | 0.945657 | 0.140794 | 0.770179 | 0.063506 | 0.945595 |

Similar set of correlation coefficients were obtained for other data sets.

## 6. Model Development and validation

The best correlated parameter pair, qs1* and $\varphi_d$ were plotted for each data set and $R^2$ value were obtained for each graph. Based on data sets resulting in $R^2$ value greater than 0.5, as given in table 4, a model is developed by plotting the two parameters collectively for all such data sets using regression approach to predict total load, as shown in Fig.1. The selected data sets are of J.P.Soni, Abdel Aal F. M., Einstein, Gibbs C.H., Nomicos, Barton & Lin, Red River (Toff) and A.M.C. Simons.

**Table 4** $R^2$ values obtained for different data sets

| S.NO. | Data Set (Lab) | $R^2$ value |
|---|---|---|
| 1 | J P Soni | 0.7904 |
| 2 | Abdel Aal F M | 0.9288 |
| 3 | Einstein H A | 0.3425 |
| 4 | Gibbs C H | 0.9928 |
| 5 | Nomicos (1956) | 0.5078 |
| 6 | Barton and Lin | 0.8486 |
| 7 | Williams G P | 0.9559 |
| 8 | RED River-Toffaletti | 0.852 |
| 9 | American Canal Simons | 0.6936 |

The proposed model is given as in eq. 12.

$$Y = 10.764\, X^{1.0565} \tag{12}$$

Where, Y represent qs1* and X represent $\varphi_d$.

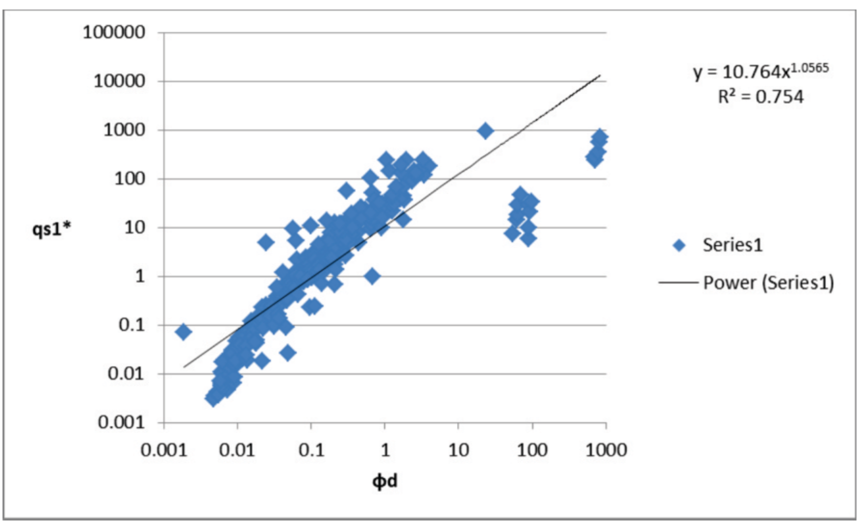


**Figure 1** Graph between qs1* and $\varphi_d$ for all the data sets

River and Rio-Grande (Nordin). The results were analysed using the statistical measure like MNE, DR and Score.

## 7. Result and Discussion

The results obtained using the proposed model for the selected lab and field data sets were analyzed using statistical measures are shown in Table 5.

**Table 5** Result of analysis using Proposed Model

| Name of Data sets | MNE | D.R | Scores ( 0.5 to 2.5 range of D.R) |
|---|---|---|---|
| Steins | -18.92 | 0.81 | 33.33 |
| Willis | 7.30 | 1.07 | 21.88 |
| Portugal River | 65.30 | 1.65 | 35.78 |
| Rio Grande- Nordin | -53.97 | 0.46 | 21.18 |

From the result of the analysis it can be seen that the MNE obtained for both lab and field data sets is between -53.97 to 65.30 which is quite good. Also the discrepancy ratio found for lab data of Willis and Steins is very close to 1.0, the ideal value, however the same for field data has variation of $\pm$ 0.5, which is also very good. The score for all data sets shows similar trend.

## 8. Conclusions

The proposed model gives extremely good results for the tested data sets. It can be concluded that dimensionless flow parameter of Duan is a dependable factor for total sediment transport prediction. Thus the proposed model can be freely applied to both lab data and field data in same format. More testing of data having different flow conditions and parameter values may be carried out by researchers even while applying the proposed model.

## References


1. Ackers, P. and white, W.R. (1973), "Sediment transport: A new approach and analysis", J. of Hydraulics Division, ASCE, 99(HY11), pp.2041–2060.
2. Bagnold, R.A. (1966), "An approach to the sediment transport problem from general physics", U.S. Geological Survey Professional Paper 422-J.
3. Brownlie, W.R. (1981), "Compilation of fluvial channel data: laboratory and field", Rep. No. KH-R-43B, W.M. Keck Lab. of Hydr. and Water Resources, California Institute of Technology,

Pasadena, Calif.
4. Colby, B.R. and Hembree, C.H. (1955), “Computations of Sediment Discharge, Niobrara River near Cody, Nebraska”. US Geological Survey Water Supply Paper 1357.
5. Duan, Jennifer G. (2013), “A simple total sediment load formula”, World Environmental and Water Resources Congress, 2013, ASCE.
6. Einstein, H.A. (1950), “The Bed Load Function in Open Channel Flows”, United States Department of Agriculture, Soil Conservation Service, Technical Bulletin No. 1026.
7. Engelund, F. and Hansen, E. (1972), A Monograph on Sediment Transport in Alluvial Streams, Teknisk Forlag, Copenhagen, Denmark.
8. Garde R J and Amraei S R S (2009), “Goncharov's total load equation”, ISH Journal of Hydraulic Engineering, Vol.15 (1), No.1, 85-100.
9. Karna Nilav et al (2015), Effect of fine sediments on river hydraulics-a research review, ISH Journal of Hydraulic Engineering, 2015, Vol. 21, No. 2, 151-161.
10. Mc. Dowell D. M. (1989), “A general formula for estimation of the rate of transport of non-cohesive bed load”, Journal of Hydraulic Research, Vol. 27, No.3, 355-361.
11. Ranga Raju K G et al (1995), “Critical evaluation of the relations for total load transport”, ISH Journal of Hydraulic Engineering, Vol. 1 (1), No.1, 37-48.
12. Samaga, B. R., Ranga Raju, K. G., and Garde, R. J. (1986 a), "Bed load transport of sediment mixtures." J. Hydr. Engrg., ASCE, 112(11), 1003-1018.
13. Samaga, B.R., Ranga Raju, K.G. and Garde R.J. (1986 b), Suspended load transport rate of sediment mixture, J. of Hydraulic Engineering, No.11, pp.1019–1038.
14. Shen, H.W., and C.S. Hung (1972), "An Engineering Approach to Total Bed-Material Load byRegression Analysis," *Proceedings of the Sedimentation Symposium,* ch. 14, pp. 14-1 through 14-1 7.
15. Shu-Qing Yang and Siow-Yong Lim (2003), Total load transport formula for flow in Alluvial channels, Journal of hydraulic engineering, Vol. 129, pg 68-72, ASCE, ISSN 0733-9429/2003
16. Shu Qing Yang (2005), “Sediment

transport capacity in rivers", Journal of Hydraulic Research, IAHR, Vol. 42, No.3, 131-138.

17. Swamee P.K and Ojha P. C (1991), Bed-load and suspended-load transport of non-uniform sediments, Journal of hydraulic engineering, vol.117, ASCE, ISSN 0733-9429/91/0006-pp No. 25868.
18. S. K. Sinnakaudan, A. Ab Ghani, M. S. S. Ahmad and N. A. Zakaria, (2006), Multiple Linear Regression Model for Total Bed Material Load Prediction, *Journal of Hydraulic Engineering*, Vol. 132, No. 5, ASCE, ISSN 0733-9429/2006/5-521–528.
19. Van Rijn, L.C. (1984 a), Sediment transport, part I: bed load transport, J. Hydr. Engi., ASCE, Vol 110, No. HY10, 1431–1456.
20. Van Rijn, L.C. (1984 b), Sediment transport, part II: suspended load transport, J. Hydr. Engi., ASCE, Vol 110, No. HY10, 1431–1456
21. Waikhom S. I & Yadav S. M. (2014), "Approaches of Total Sediment Transport of Alluvial River: The State of the Art", International journals of Scientific Engineering and Technology, ISSN-2277-1581, pg-377.
22. White, W.R., H. Milli and A.D. Crabbe (1973), Sediment Transport: An Appraisal of Available Methods. Vol. 2, Report No. INT 119, Hydraulics Research Station, Wallingford, England, Nov.
23. Wu W. Wang S.S.Y. and Jia Y. (2000), Non-uniform sediment transport in alluvial rivers,Journal of Hydraulic Research, IAHR, Vol..38, No6
24. Yang C.T. (1979), Unit Stream Power Equation for Total load, Journal of Hydraulic Engineering, ASCE, (40) 12, pp. 123-138.
25. Yang C.T. (2002), Sediment Transport and Stream Power, International Journal of Sediment Research, vol. 17, no. 1, Beijing, China, pp. 3 1-38.
26. Chanson, H. (1999), "The hydraulics of open channel flow", New York, John Wiley & Sons.
27. Garde R. J., 1995, History of Fluvial Hydraulics, New Age International (P) Limited, New Delhi, India.
28. Garde R. J, K. G. Ranga Raju 2006, Mechanics of Sediment Transportation and Alluvial Stream Problems, Third Edition, New age Publication, New Delhi.
29. Graf W.H. (1971), Hydraulics of sediment transport, McGraw Hill, New York.

# Instructions for Authors

**Essentials for Publishing in this Journal**

- Submitted articles should not have been previously published or be currently under consideration for publication elsewhere.
- Conference papers may only be submitted if the paper has been completely re written (taken to mean more than 50%) and the author has cleared any necessary permission with the copyright owner if it has been previously copyrighted.
- All our articles are refereed through a double-blind process.
- All authors must declare they have read and agreed to the content of the submitted article and must sign a declaration correspond to the originality of the article.

**Submission Process**

All articles for this journal must be submitted using our online submissions system. http://enrichedpub.com/ . Please use the Submit Your Article link in the Author Service area.

---

**Manuscript Guidelines**

The instructions to authors about the article preparation for publication in the Manuscripts are submitted online, through the e-Ur (Electronic editing) system, developed by **Enriched Publications Pvt. Ltd**. The article should contain the abstract with keywords, introduction, body, conclusion, references and the summary in English language (without heading and subheading enumeration). The article length should not exceed 16 pages of A4 paper format.

**Title**

The title should be informative. It is in both Journal's and author's best interest to use terms suitable. For indexing and word search. If there are no such terms in the title, the author is strongly advised to add a subtitle. The title should be given in English as well. The titles precede the abstract and the summary in an appropriate language.

**Letterhead Title**

The letterhead title is given at a top of each page for easier identification of article copies in an Electronic form in particular. It contains the author's surname and first name initial .article title, journal title and collation (year, volume, and issue, first and last page). The journal and article titles can be given in a shortened form.

**Author's Name**

Full name(s) of author(s) should be used. It is advisable to give the middle initial. Names are given in their original form.

**Contact Details**

The postal address or the e-mail address of the author (usually of the first one if there are more Authors) is given in the footnote at the bottom of the first page.

**Type of Articles**

Classification of articles is a duty of the editorial staff and is of special importance. Referees and the members of the editorial staff, or section editors, can propose a category, but the editor-in-chief has the sole responsibility for their classification. Journal articles are classified as follows:

**Scientific articles:**

1. Original scientific paper (giving the previously unpublished results of the author's own research based on management methods).
2. Survey paper (giving an original, detailed and critical view of a research problem or an area to which the author has made a contribution visible through his self-citation);
3. Short or preliminary communication (original management paper of full format but of a smaller extent or of a preliminary character);
4. Scientific critique or forum (discussion on a particular scientific topic, based exclusively on management argumentation) and commentaries.

Exceptionally, in particular areas, a scientific paper in the Journal can be in a form of a monograph or a critical edition of scientific data (historical, archival, lexicographic, bibliographic, data survey, etc.) which were unknown or hardly accessible for scientific research.

**Professional articles:**

1. Professional paper (contribution offering experience useful for improvement of professional practice but not necessarily based on scientific methods);
2. Informative contribution (editorial, commentary, etc.);
3. Review (of a book, software, case study, scientific event, etc.)

**Language**

The article should be in English. The grammar and style of the article should be of good quality. The systematized text should be without abbreviations (except

standard ones).
All measurements must be in SI units. The sequence of formulae is denoted in Arabic numerals in parentheses on the right-hand side.

**Abstract and Summary**

An abstract is a concise informative presentation of the article content for fast and accurate Evaluation of its relevance. It is both in the Editorial Office's and the author's best interest for an abstract to contain terms often used for indexing and article search. The abstract describes the purpose of the study and the methods, outlines the findings and state the conclusions. A 100- to
250- Word abstract should be placed between the title and the keywords with the body text to follow. Besides an abstract are advised to have a summary in English, at the end of the article, after the Reference list. The summary should be structured and long up to 1/10 of the article length (it is more extensive than the abstract).

**Keywords**

Keywords are terms or phrases showing adequately the article content for indexing and search purposes. They should be allocated heaving in mind widely accepted international sources (index, dictionary or thesaurus), such as the Web of Science keyword list for science in general. The higher their usage frequency is the better. Up to 10 keywords immediately follow the abstract and the summary, in respective languages.

**Acknowledgements**

The name and the number of the project or programmed within which the article was realized is given in a separate note at the bottom of the first page together with the name of the institution which financially supported the project or programmed.

**Tables and Illustrations**

All the captions should be in the original language as well as in English, together with the texts in illustrations if possible. Tables are typed in the same style as the text and are denoted by numerals at the top. Photographs and drawings, placed appropriately in the text, should be clear, precise and suitable for reproduction. Drawings should be created in Word or Corel.

**Citation in the Text**

Citation in the text must be uniform. When citing references in the text, use the reference number set in square brackets from the Reference list at the end of the article.

**Footnotes**

Footnotes are given at the bottom of the page with the text they refer to. They can contain less relevant details, additional explanations or used sources (e.g. scientific material, manuals). They cannot replace the cited literature.
The article should be accompanied with a cover letter with the information about the author(s): surname, middle initial, first name, and citizen personal number, rank, title, e-mail address, and affiliation address, home address including municipality, phone number in the office and at home (or a mobile phone number). The cover letter should state the type of the article and tell which illustrations are original and which are not.